ACS APPLIED POLYMER MATERIALS

pubs.acs.org/acsapm Review

# Polymeric Particulates of Controlled Rigidity for Biomedical Applications

Veronika Kozlovskaya, Maksim Dolmat, and Eugenia Kharlampieva*

Cite This: *ACS Appl. Polym. Mater.* 2021, 3, 2274–2289 Read Online

ACCESS | Metrics & More | Article Recommendations

**ABSTRACT:** The mechanical stiffness of polymer particles is an important parameter that influences particle circulation in the blood and governs cell–particle adhesion, cellular uptake, and biodistribution. This Review highlights the main approaches to produce micro and nanosized polymeric particulates with controlled mechanical responses and their applications in the biomedical field. We discuss how varying mechanical properties of polymeric particles can affect particle interactions with various types of cancer and immune cells, along with particle behavior in the flow. We also analyze the possibilities of regulating particle rigidity by controlling particle shape, a relatively unexplored research area. The main measurement methods to test the mechanical responses of polymeric particulates are also reviewed. Finally, we summarize recent developments toward controlling the mechanical responses of polymeric particulates relevant to biomedical applications and highlight important perspective directions that can advance fundamental and applied research in this area.

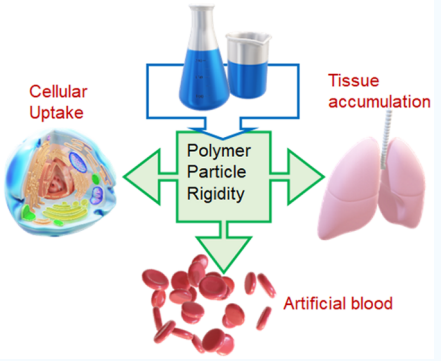


**KEYWORDS:** *rigidity, shape, polymeric particles, biomedical applications, elastic modulus, particle stiffness*



## 1. INTRODUCTION

The mechanical properties of polymer particles intended for *in vivo* applications are important parameters that influence particle circulation in the blood and govern cell–particle adhesion, cellular uptake, and biodistribution.[1−4] Therefore, a better understanding of the ways to produce polymer particles with controlled mechanical properties is crucial for developing viable nano- and microparticle theranostic vehicles.

In response to applied stress and mechanical deformations, polymers exhibit viscoelastic mechanical responses, which can vary with the time and frequency of the deformation.[5] The polymer particle's resistance to applied pressure is characterized by the bulk modulus. The ability to resist deformation while under stress is defined as the material's rigidity.[1] When the material can subsequently return to its original size/shape upon stress release, it is considered elastic. The material's response as strain ($\gamma$) to linear stress ($\sigma$) is related through Young's modulus, $E = \sigma/\gamma$, which is the intrinsic mechanical property of a material. The particle stiffness is directly proportional to the elastic modulus for a given particle dimension, and larger values of Young's modulus characterize stiffer materials that are more difficult to compress and elongate.[6]

Most current approaches to control the rigidity of polymeric particles focus on the mechanical properties of the materials that can be regulated by the choice of the polymer or by varying the material's cross-link density.[1,7] Conversely, the consideration of mechanical properties of particles as objects can also be useful to control the mechanical behavior of polymeric particulates. In this case, the mechanical properties of polymer objects can depend on particle shape (spherical or nonspherical), size, and morphology (particle architecture such as filled, porous, or hollow or surface properties).

To vary particle architecture, a variety of emulsion methods from preformed polymers and the polymerization of monomers (emulsion and interfacial) have been developed for the synthesis of filled or hollow polymer particles. Simultaneously, template-assisted layer-by-layer (LbL) assembly can be used to fabricate hollow polymeric capsules of any size, geometry, and thickness controlled at the nanoscale via alternating the deposition of the polymers at the solid/liquid interfaces.[8−12] The LbL technique can easily impart a desired elasticity and responsiveness to the nanothin capsule wall by selective control over the shell chemistry through polymer selection, polymer molecular weight, shell thickness, and degree and type of cross-linking.[13−16] To produce polymer particles of well-defined nonspherical geometries, a range of shape engineering technologies, including particle replication in nonwetting template (PRINT),[17] stretching of films with

Received: February 2, 2021
Accepted: April 13, 2021
Published: April 22, 2021

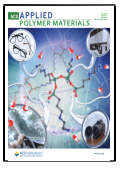




https://doi.org/10.1021/acsapm.1c00157
*ACS Appl. Polym. Mater.* 2021, 3, 2274–2289

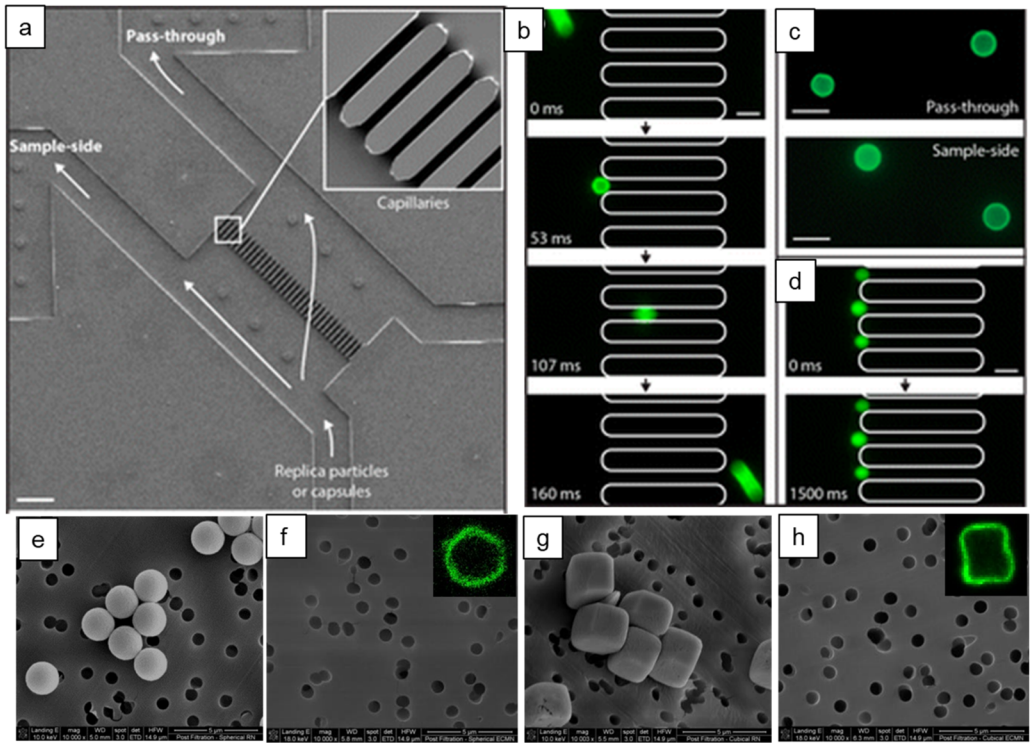


**Figure 1.** (a) Scanning electron microscopy (SEM) image of a microfluidic model of a blood capillary. The arrows show flow paths for spherical polymeric microparticles in the device. (b, c, d) Fluorescence microscopy images of microparticles flown through the device's capillaries. Scale bars are 100 $\mu$m (a) and 10 $\mu$m (b–d). Reprinted from ref 33. Copyright 2015 American Chemical Society. SEM images of extravasation (filtration) tests of spherical (e, f) and of cubical (g, h) rigid core–shells (e, g) and soft shells (f, h) of hydrogen-bonded multilayer microcapsules through the 0.8 $\mu$m pores. The insets in (f, h) are the confocal scanning microscopy images of the shells that passed through the pores and maintained their initial spherical (f) or cubical (h) shape. Reprinted with permission from ref 35. Copyright 2015 Wiley and Sons.

embedded polystyrene spheres,[18] and template-induced printing,[19] have been developed.

The use of polymer hydrogels, hydrophilic networks of cross-linked macromolecules, can allow for the mimicry of the rigidity of biological objects such as viruses, bacteria, and cells and for the facile regulation of biological activity of the hydrogel particles, their association with cancer cells, and the accumulation in targeted sites due to their large volume changes in water.[1,20−23] For example, a decrease in the elastic modulus of poly(ethylene glycol) (PEG) nanogels from 3000 to 10 kPa increased their *in vivo* circulation up to 2 h.[23] A reduction in the elastic modulus of PRINT hydrogel microparticles 8-fold led to a 30-fold increase in the circulation half-life.[24] Unlike hydrogels, the highly cross-linked microsized networks obtained by microfluidics, lithography, and PRINT, while offering excellent control over shape, often lack capabilities toward swelling in aqueous media.[25,26]

In this respect, multilayer hydrogel capsules obtained through LbL assembly are capable of large volume transitions and the fast reversibility of the responses. Unlike bulk microscopic networks, hydrogel microcapsules have much larger free volume due to the capsule interior, and because the swelling rate is inversely proportional to the square of the network dimensions,[27] the nanoscale capsule hydrogel wall can produce a much faster response than microscopic hydrogel materials.

Given the importance of rigidity for particle behavior, this Review highlights recent developments in the field of soft polymer particulates with controlled mechanical responses and their applications in the biomedical field. We summarize the main methods and approaches toward varying the rigidity of polymeric particles by material choice, hydrogel cross-link density, and hydration. We also analyze the possibilities of regulating particle rigidity by controlling particle shape, a relatively new and unexplored research area. We discuss how the rigidity can impact particle interactions with various cancer and immune cells and their behavior in the flow. Examples of existing and emerging instrumental techniques for testing mechanical responses of polymeric particulates are also reviewed. Finally, we highlight essential perspective directions that can advance fundamental research in the field of polymer particulates, which could further expand material biomedical applications.

## 2. MEASUREMENT METHODS OF POLYMER PARTICLE MECHANICAL RESPONSES

Herein, we briefly describe the measurement methods and quantification of particle mechanical properties. For a comprehensive review on molecular characterization methods of polymer networks including networks mechanics and dynamics, the readers are referred to a recent review by Rubinstein and colleagues.[5]

### 2.1. Quantification of Particle Mechanical Properties.

Mechanical properties of polymeric nanoparticles are often characterized by (a) Young's modulus ($E$), which is the slope of the stress–strain curve in the elastic (reversible) deformation regime; (b) shear modulus ($G$), the ratio between shear stress and shear strain; (c) bulk modulus ($K$), which characterizes the change in particle volume upon the pressure


https://doi.org/10.1021/acsapm.1c00157
ACS Appl. Polym. Mater. 2021, 3, 2274−2289

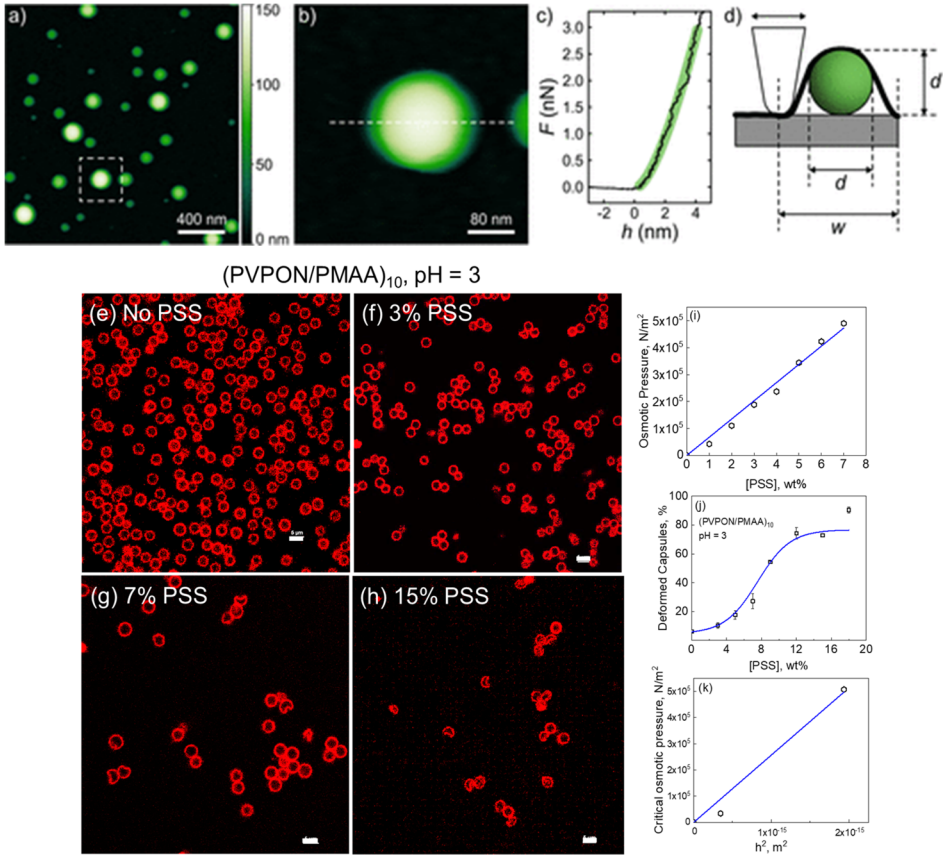


**Figure 2.** Using AFM nanoindentation, the elastic modulus of a polymer nanoparticle $E$ is obtained by first collecting a topography image to identify individual particles (a), followed by a high-resolution topography analysis of an isolated particle (b). Force curves are collected with force $F = f(h)$, where $h$ is indentation; the linear slope is the contact model fit from which the elasticity modulus is obtained (c). (d) Schematics show the path (solid black line) of an AFM tip scanning across a particle. (d) Geometrical parameters of the particle can be derived from image analysis to determine the AFM tip diameter. Reprinted from ref 43. Copyright 2020 American Chemical Society. The osmotic pressure difference method for the elastic modulus of spherical multilayer capsules included the analysis of confocal microscopy images (e–h) exposed to PSS solutions with different concentrations. Scale bar is 5 $\mu$m in (e–h). Calibration curve for the osmotic pressure induced with various concentrations of PSS sodium salt (i). The calculation of the percentages of deformed capsules as a function of PSS concentration (j), and the determination of the critical osmotic pressure as a function of the capsule wall thickness (k). Reprinted from ref 47. Copyright 2019 American Chemical Society.

change.[28] These moduli correlate between each other through Poisson's ratio, $\nu$ (1):[28]

$$2G(1 + \nu) = E = 3K(1 - 2\nu) \quad (1)$$

The stiffness of a particulate can be characterized by the elastic deformation and shows the ratio of applied force and a corresponding length change. It is often used for polymeric particles mimicking biological material, such as red blood cells (RBCs), to describe their softness and ability to deform in the bloodstream.[33,29] Shear elastic modulus ($G$) of polymeric microparticles can be obtained in microfluidic experiments upon particles passing through capillaries with physiologically appropriate dimensions and pressure.[30,31]

**2.2. Particle Deformability.** The methods to observe the deformability of polymeric carriers in the flow include an observation of the particles passing through narrow microfluidic channel capillaries (*in vitro*)[32−34] (Figure 1a–d) or through blood capillaries (*in vivo*) using optical and confocal microscopy.[54] The data can be analyzed as the ratio of the pass-through to the total particles fed to the channel. Particle deformability can be also evaluated using filtration measurements[35,71] (Figure 1e–h) and micropipette aspiration tests.[36] In the former case, the particle suspension is filtered through a membrane with a known pore size by applying a certain pressure, which serves as the measure of particle rigidity.[35] In the latter, the degree of particle deformation can be evaluated through selected geometrical parameters, *e.g.*, particle volume.[37] In this case, the particle mechanical response can be characterized by complete recovery of the material's original shape, whereas a plastic response is accompanied by a permanent change of the material's shape, *e.g.*, irreversible capsule buckling or capsule rapture.[32]

Using a PDMS microfluidic device with a narrowing within the main channel that mimicked the geometry of wide and narrow blood vessels, Kumacheva and co-workers studied the mechanical behavior of agarose spherical microgels with diameters ranging from 40 to 140 $\mu$m and Young's moduli in the range from 2.6 to 20.2 kPa being confined to the microfluidic channel.[38] The authors developed a quantitative model for microgel volume changes due to a uniform compression of a microgel upon the microgel's entering a microfluidic channel tightening. They showed that, for each set of microchannel geometrical parameters (an entrance angle of the narrowing), experimental parameters including microgel diameter, a diameter of the narrowing inside the main channel, Young's modulus of a microgel, and a translocation pressure (the pressure difference required for a microgel to move through the channel narrowing) could be combined into a set


https://doi.org/10.1021/acsapm.1c00157
ACS Appl. Polym. Mater. 2021, 3, 2274−2289

of curves that can be used to measure the elasticity modulus of a microgel with unknown rigidity by measuring its translocation pressure as a function of the confinement degree.[38]

**2.3. Small Particle Deformations.** The AFM nanoindentation method can be used to characterize the mechanical properties of polymeric carriers using small deformations.[28,39] During the experiment, the force curve is obtained by measuring the sample's deformation with the AFM cantilever driven down onto the sample at a known force (Figure 2a–d).[40] To obtain reliable data, one must consider the shape and stiffness of the cantilever. While sharp conical tips of a nanometer size are mostly used for topographical imaging, colloidal probes, *i.e.*, AFM cantilevers with an attached sphere of micrometer size, are best suited for the mechanical characterization of soft nanomaterials.[41] Since colloidal probes have a large contact area, it is impossible to measure local differences in mechanical properties within the particle, and the entire stiffness of the particle is measured instead. The use of sharp tips allows for high-resolution topographical imaging and simultaneously collects mechanical properties of soft polymer particles; however, their high adhesiveness can pose experimental challenges.[42] For characterization of mechanical behavior of soft particulates in the physiologically relevant media (buffered saline, 37 °C), special equipment and expertise might be required.[43]

**2.4. Large Particle Deformations.** Bulk modulus ($K$) can be calculated from the large deformations of the polymeric shells under known osmotic pressure differences. When one considers that the particle shell is impermeable to molecules with a high molecular weight and permeable to small molecules like a solvent, an osmotic pressure difference can be induced by placing the shells in a high molecular weight polymer solution at various concentrations. As demonstrated for polyelectrolyte multilayer capsules,[16,44,45] the spherical capsule loses its shape and transforms from a convex shape to a concave inward buckled shape when the work done by the external pressure equals the deformation energy, from which the critical pressure for the onset of capsule buckling is obtained (Figure 2e–k). The buckling of multilayer spherical capsules induced by polystyrene sulfonate sodium salt (PSS) is due to the isotropic osmotic pressure difference between inside and outside of the multilayer shell.[46] Capsule buckling can be monitored by optical or confocal fluorescence microscopy.

When the osmotic pressure of the solution exceeds that of the capsule interior, the solution is squeezed out if the shell's elastic force cannot compensate for the rising pressure difference.[46] To convert shell deformation into bulk modulus, a sigmoidal curve of the percentage of deformed particles versus the polymer solution concentration is plotted. The osmotic pressure difference corresponding to the concentration at which 50% of the particle is deformed is considered the critical osmotic pressure. The osmotic pressure calibration curves for a specific macromolecule concentration are obtained by vapor pressure reduction using a vapor pressure osmometer. The elasticity modulus, $E$, of the capsule wall is related to the critical pressure difference ($P_c$) through the following expression (2):

$$P_{cr} = \frac{2E}{\sqrt{3(1-\nu^2)}}\left(\frac{\delta}{R}\right)^2 \quad (2)$$

where $\nu$ is the Poisson's ratio, $\delta$ is the shell's thickness, and $R$ is the particle's radius.[46,47]

It is often beneficial to employ various techniques for the characterization of the mechanical behavior of the particulate to elucidate the possible effects from various structural parameters such as, for example, the internal structure of the particulates made from the same material. For example, Sun et al. utilized both AFM nanoindentation in buffer solution using colloidal cantilevers and the microfluidic model to analyze hyaluronic acid (HA) hollow capsules and HA porous polymeric particles of 7 $\mu$m that were obtained through the continuous assembly of polymers mediated by atom transfer radical polymerization.[33] Both HA capsules and particles showed similar stiffness in the range from ∼4 to ∼13.6 mN $m^{-1}$ and ∼2.4 to ∼21.3 mN $m^{-1}$, respectively, by either increasing the capsule thickness or varying HA density by changing the amount of methacrylate-functionalized HA reagent. Despite that, the capsules and particles showed a different behavior in the flow. All capsules showed reversible elastic deformation when passing through the microfluidic channels. Simultaneously, the particles exhibited a lack of deformability and had a difficulty traversing through the microcapillaries at a wide range of pressure even when the particle stiffness was 6-fold lower than that of the capsules.

Conversely, Doshi et al. fabricated multilayer RBC-shaped microcapsules of PSS/hemoglobin (PSS/Hb) and compared their mechanical properties with mouse RBCs by both AFM nanoindentation and microfluidic tests.[48] Although they found a 6-fold difference in the elastic modulus between the microcapsules (92.8 ± 42 kPa) and the RBCs (15.2 ± 3.5 kPa), the capsules demonstrated deformability similar to the RBCs when passing through a 5 $\mu$m glass capillary.[48]

In another example, highly soft PEG hydrogel microparticles with a Young's modulus ranging from 0.2 to 3.3 kPa were obtained by varying the hydrogels' cross-link density.[30] However, despite being on average much softer (3.3 kPa) than the RBCs (26 kPa), only PEG hydrogels with the lowest cross-linking degree were able to reversibly deform while passing through the capillaries and restore their initial shape when they came out of the channels.[30]

## 3. PARTICLE RIGIDITY CONTROLS PARTICLE INTERACTIONS WITH CELLS

Different types of cells, including immune cells, have been shown to internalize particulates depending on the particle size ranging from 30 nm to 5 $\mu$m with decreased phagocytosis outside this range.[49−52] However, many studies suggest that the particulates' rigidity is among the key factors that control particle interactions with the cells.[23,53−55] In this respect, the varying elastic modulus of the particles can be used to increase their circulation time, avoid macrophage clearance or, conversely, induce the uptake of particles by antigen-presenting immune cells for more efficient vaccines and improve the targeting drug delivery.[1] To control the internalization of particles by various cells, it is essential to understand how the softness/rigidity of a polymer particle correlates with its intracellular trafficking. When a polymer carrier is taken up by a cell, it is moved inside the cell being compartmentalized by a lipid bilayer membrane of the intracellular vesicle. The particle needs to escape from these endosomal/lysosomal compartments into cytosolic space or other intracellular organelles without compromising cell function to induce a therapeutic effect. When one understands how a polymeric carrier's rigidity affects its intracellular transport, its therapeutic efficiency can be improved. A better


https://doi.org/10.1021/acsapm.1c00157
ACS Appl. Polym. Mater. 2021, 3, 2274−2289

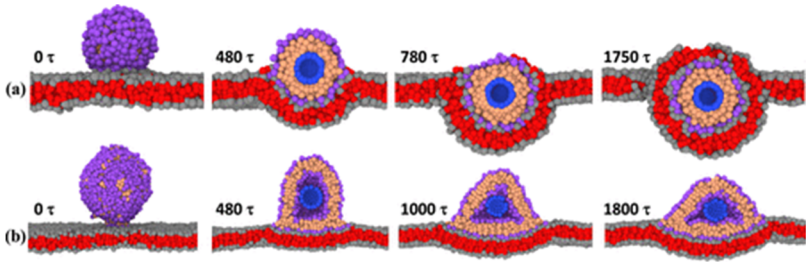


**Figure 3.** MD simulation of endocytosis for (a) rigid and (b) soft spherical nanoparticles. Rigid and soft particles of the same volume are shown to internalize differently. The higher energy barrier needs to be overcome for soft particles due to their deformation. Reprinted from ref 65. Copyright 2019 American Chemical Society.

understanding of the effects of a carrier's mechanical clues on the regulation of various biological phenomena is vital to enable the development of polymeric carriers with tunable mechanical behavior. The effects of the particulate's rigidity on cell−particle interactions can be drastically different and depend on the particle material, size, and shape, presence of protein corona, cell type, and particle uptake mechanism.[53,56] Herein, we highlight biological phenomena that can be affected by particle rigidity and are essential for outlining novel design criteria that can be used to advance the development of more effective polymeric carriers.

**3.1. Particle Rigidity Affects Cellular Internalization.** Many reports suggest a better cellular uptake of more rigid particulates. For example, Nowak et al. showed that rigid polystyrene particles of 200 nm with a Young's modulus of 3 GPa were 10-fold better associated with and transported through the *in vitro* endothelial cell membrane than soft 200 nm PEG diacrylate (DA) hydrogel particles that had a 1000-times lower Young's modulus,[57] although the observed difference could be partly attributed to their different adhesive interactions due to the PEG hydrophilicity and antiadhesive nature. Conversely, the *in vitro* cellular uptake of 200 nm hydrogels with a Young's modulus of 10 and 3000 kPa obtained by PEGDA polymerization demonstrated that the rigid PEG hydrogels were internalized to a greater extent and faster than the softer hydrogels by 4T1 epithelial tumor cells and bEnd.3 brain epithelial cells within a 12 h incubation. In the case of J774 macrophages, rigid hydrogels were taken up by the phagocytes even faster and in larger quantities than the softer hydrogels.[53]

Similarly, rigid (∼25 kPa) mesoporous hydrogel particles of cross-linked poly(L-glutamic acid) synthesized by the mesoporous silica-templated assembly for the delivery of oligonucleotide CpG adjuvant (800 nm) associated more with human plasmacytoid dendritic cells (DCs) than their softer (∼2 kPa) counterparts after a ∼10 h incubation at 37 °C.[58] The increased uptake of rigid polymeric carriers over softer counterparts was also found for zwitterionic nanogels by epithelial cells,[59] hydrogen-bonded multilayer capsules by macrophages,[60] hydrogel poly(allylamine hydrochloride) PAH capsules by smooth muscle cells,[61] composite multilayer capsules by placental cells,[62] nanoliposomal gels by MDA-MB-231 and MCF-7 human breast cancer cells,[63] and block copolymer micelles by A375 tumor cells.[64]

Zhang and co-workers applied coarse-grained molecular dynamics (MD) to simulate the results of membrane internalization of gold nanoparticles coated with lipid layers of varied thickness to modulate the particle softness. Molecular simulations of these lipid-coated gold beads having the same size of ∼60 nm revealed that the softer particles exhibited ∼60% lower internalization by 4T1 murine mammary carcinoma cells after a 4 h incubation because of the larger free energy barrier required to be overcome for softer beads during the internalization by the cell membrane (Figure 3).[65]

Studies on the effects of particle rigidity on permeation through biological hydrogels, *i.e.*, mucus, explored spherical poly(lactic-*co*-glycolic) (PLGA) particles coated with a lipid bilayer. The particle rigidity was controlled by the amount of water between the PLGA core and the lipid coating.[66,67] When the PLGA core size increased from 50 to 160 nm, the water layer thickness decreased, and core−shells with soft (5 MPa), semisoft (50 MPa), and rigid (110 MPa) structures were obtained. The studies found that the effective diffusivity in mucus was the fastest for the semielastic core−shells, while it was impeded for soft and rigid structures. The coarse-grain MD simulation of these particle diffusivities through a network of polymer fibers suggested that soft core−shells would undergo excessive deformation and interact with the matrix via physical entanglement and increased adhesion.[66,67] In contrast, the superior diffusivity of the semielastic core−shells was due to their moderate stiffness, resulting in the particle deformation into ellipsoids and increasing their rotational movement and translational diffusion through the network.

In a recent example, however, a Pickering emulsion droplet's high deformability, *i.e.*, the particle's ability to reversibly change shape by cellular wrapping, resulted in a large contact area with a cell membrane, which induced enhanced interactions with antigen-presenting cells and led to potent immune responses.[68] These overall findings demonstrate the importance of the interplay between particle mechanical response, shape, and cell type, which is often too complex to decouple.

**3.2. Particle Rigidity Affects Tissue Accumulation.** Unlike rigid particles, the longer circulation half-life of the softer counterparts due to the evasion of professional phagocytic immune cells can be favorable for increasing their probability of passing through tumor vasculature with lower flow and favorable vascular adhesion. In this respect, softer polymeric carriers can facilitate better tissue accumulation. For example, in the *in vivo* experiments with tumor models obtained from human primary glioblastoma cells (U87-MG) (a brain tumor model) and melanoma cells (B16-F10) (a model for skin cancer), Decuzzi and co-workers demonstrated a 6-fold higher tumor accumulation of soft discoidal polymer constructs unlike their rigid counterparts with mechanical stiffness of 1.3 and 15 kPa, respectively, after 24 h of circulation in blood.[54] The constructs were obtained by UV-cross-linking of a mixture combining PLGA, PEGDA, lipid-


https://doi.org/10.1021/acsapm.1c00157
ACS Appl. Polym. Mater. 2021, 3, 2274−2289

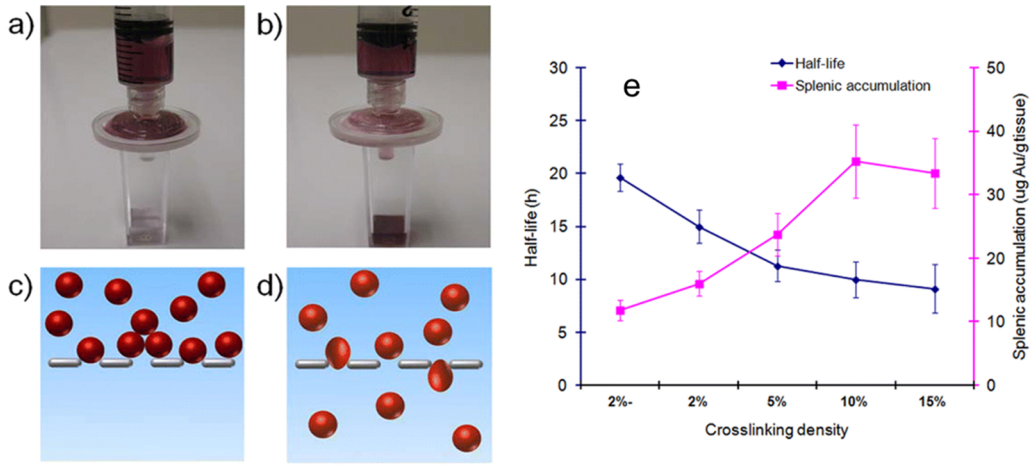


**Figure 4.** Photographs of rigid (a) and soft (b) zwitterionic nanogels (0.25 $\mu$m) passing through 0.22 $\mu$m pores. Schematics show that the rigid nanogels (c) are filtered off, while the soft ones (d) pass through the pores due to deformability. (e) Circulation half-life decreases, and accumulation in the spleen increases with the increased cross-link density of the nanogels. Reprinted from ref 71. Copyright 2012 American Chemical Society.

tetraxetan (DOTA), lipid-Rhodamine B, and 20 nm iron oxide nanocubes.[54]

In another study with the discoidal polymeric constructs of circular, ellipsoid, and quadrangular shapes and Young's modulus varied over the range from 100 kPa to 10 MPa as analyzed by AFM nanoindentation, Decuzzi and co-workers suggested that there was a relationship between the particle bending stiffness and internalization by professional phagocytic cells.[4] According to their findings for the discoidal polymeric particles, the softer ones with $Eh^3$ ($E$ is Young's modulus, $h$ is the particle thickness) slightly lower than that of the cells will be far less internalized than those stiffer than that threshold. Similarly, hydrogel particles (170 nm) of intermediate elasticity were internalized more than those much softer or much stiffer.[69]

The softer and more deformable microparticles derived from tumor-repopulating cells were shown to exhibit enhanced tumor accumulation because of their ability to easily deform and extravasate from the blood vessel into a surrounding tumor tissue through the gaps between the endothelial cells in leaky cancerous vasculature.[70] Similarly, the softer zwitterionic hydrogels of cross-linked poly(carboxybetaine) also easily passed through the splenic filtration because of large deformability, unlike their stiffer counterparts, which led to their longer circulation time and low accumulation in the spleen (Figure 4).[71]

The deformability of softer particles compared to the rigid ones was also suggested by a computational study by Coclite et al. to be beneficial in resisting perturbations in the blood flow.[72] The work demonstrated that, while rigid particles can be easily detached from the capillary walls by circulating blood cells because of the short-lived adhesion of rigid particles, their softer counterparts can deform and convert some kinetic energy from circulating cells into elastic energy. Thus, their firm attachment to the capillary walls would favor a long-sustained release of drugs into the tissue.

**3.3. Particle Deformations upon Interactions with Cells.** Several works suggested an exciting approach to probe mechanical forces exerted on polymer particles during cellular uptake.[73,74] For example, when Palankar et al. observed the deformation of poly(styrenesulfonate)/PAH (PSS/PAH) multilayer capsules by cells using live-cell imaging,[74] they found that the deformation of a 4-layer PSS/PAH microcapsule begins during its uptake by the HeLa cells when the microcapsule is just attached to the cell membrane. The capsule enveloping by the phagosomal cup was gradually buckled and deformed upon the internalization. The thicker, 8- and 12-layer microcapsules were also deformed, and their cargo was released during the cellular uptake.

To correlate the deformation of poly(diallyldimethylammonium chloride)/PSS multilayer capsules during cellular internalization with the mechanical force exerted by Vero cells, Delcea and co-workers used AFM nanoindentation.[74] The degree of plastic deformation of the microcapsules corresponded to the force of at least 0.2 $\mu$N during cell internalization of the capsules.

It was suggested that, while AFM nanoindentation uses an anisotropic local force to the particles, the isotropic compression can allow a more realistic model for imitating intracellular mechanical forces. Thus, Caruso and co-workers quantified the pressures exerted by cells upon the internalization of soft multilayer hydrogel capsules of poly(methacrylic acid) (PMAA) using an *ex vivo* osmotic pressure difference approach.[73] They found that the internalization of PMAA hydrogel capsules by human monocyte-derived macrophage THP-1 cells induces the pressure of 357 ± 13 kPa. Different types of cells also induced different pressures upon the internalization of particles.[75] For example, the percent of PMAA multilayer hydrogel capsules deformed upon cellular uptake was 96% for HeLa human epithelial cells, 56% for RAW264.7 mouse macrophage cells, and 29% for differentiated THP-1 macrophage cells, indicating greater forces exerted by the HeLa cells.[75]

Therefore, understanding cell mechanobiology and mechanical forces exerted by different cell lines during the uptake of polymer carriers is critical for designing intelligent delivery vehicles for the controlled interaction with various biological tissues.

## 4. APPROACHES TO REGULATE THE RIGIDITY OF POLYMERIC PARTICLES

The achievement of environmental control over the particulate's rigidity is among the key parameters in developing the


https://doi.org/10.1021/acsapm.1c00157
ACS Appl. Polym. Mater. 2021, 3, 2274−2289

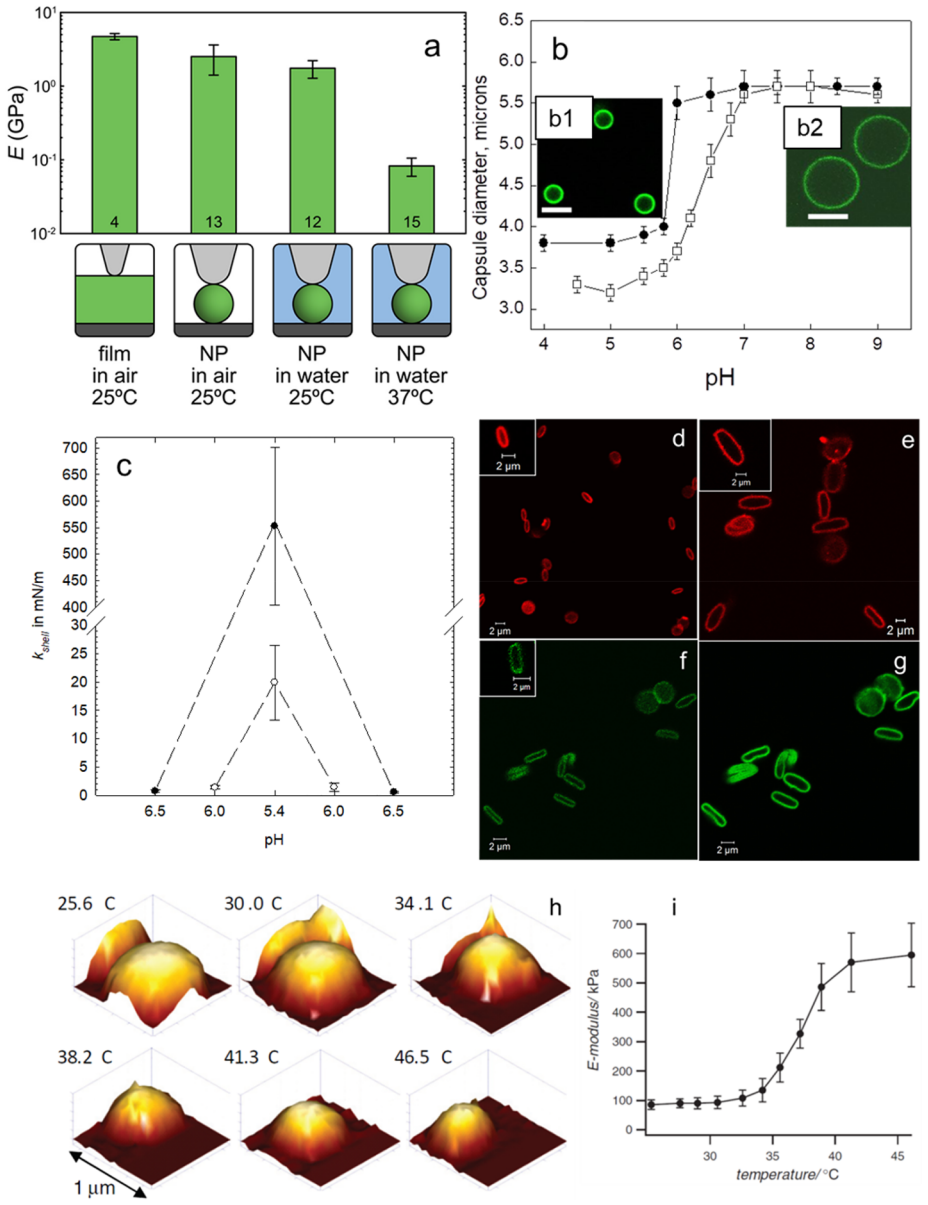


**Figure 5.** (a) Elastic modulus for PLA particles measured for bulk film, particles in the air, water at 25 °C, and water at 37 °C. Reprinted from ref 43. Copyright 2020 American Chemical Society. (b) pH-dependent size of multilayer hydrogel capsules with their CLSM images at pH = 4.5 (b1) and pH = 8 (b2). Reversible stiffening of the hydrogel at pH changes from 6.5 to 5.4 (c). Reprinted with permission from ref 93. Copyright 2006 The Royal Society of Chemistry. CLSM images of discoidal 15-layer PMAA (d, e) and 5-bilayer PMAA/poly(*N*-vinylpyrrolidone) (PVPON) (f, g) hydrogel capsules at pH = 4 (d, f) and pH = 7.4 (e, g). More rigid PMAA/PVPON capsules swell less at the high pH and shrink less at the low pH than PMAA capsules. Reprinted from ref 88. Copyright 2014 American Chemical Society. AFM topography three-dimensional images of the PNIPAM microgel at varied temperatures (h) and their temperature-dependent Young's moduli (i). Reprinted with permission from ref 76. Copyright 2010 Wiley and Sons.

next generation of "intelligent" materials capable of mechanical transformations to perform desired functions. This capability of switching rigidity of a polymeric carrier can be of great use in biomedical technologies. For instance, switching the stiffness of surfaces has been reported to control cells' behavior to regulate cellular adhesion.[76,77] Herein, we highlight the main approaches to control the rigidity of polymeric carriers using hydration, cross-link density, stimuli responses including pH and temperature, and geometrical features including shape and architecture.

**4.1. Hydration.** Alsharif et al. used AFM indentation analysis of poly(lactic acid) (PLA) and PLGA nanoparticles to study the influence of water on the mechanical properties of the nanoparticles.[43] They demonstrated the 30-fold reduction in the nanoparticles' elastic modulus in water at 37 °C because of the water plasticizing effect on the polymer glass transition temperature (Figure 5a). To study the effect of hydration on particles, two samples, PLA and PLA/PLGA (50:50) nanoparticles prepared by nanoprecipitation, were tested under dry and wet conditions. The elastic modulus for the PLA particles decreased from 2.5 ± 1.1 GPa in the dry state to 83 ± 23 MPa in the hydrated state at 37 °C. A similar trend was observed for PLGA nanoparticles with the decrease in the elastic modulus from 2.9 ± 0.7 GPa in the dry state to 58 ± 30 MPa in the hydrated state. Despite this simple approach to decrease Young's modulus of polymeric nanoparticles, the rigidity of


https://doi.org/10.1021/acsapm.1c00157
ACS Appl. Polym. Mater. 2021, 3, 2274−2289

relatively more hydrophilic PLGA particles was still in the MPa range, which is significantly stiffer than that for many biological tissues that exhibit elasticity in the kPa range.[78,79]

The regulation of the hydrogel particles' fluid content (the hydration degree of a hydrogel) is also the simplest way to tune the hydrogel elasticity.[80] Thus, poly(*N*-isopropylacrylamide) (PNIPAM) nanogels synthesized by surfactant-free radical polymerization in water and analyzed by AFM nanoindentation showed a 63-fold decrease in their elastic modulus upon hydration.[81] The modulus for the PNIPAM spheres in water was 1.8 ± 0.2 MPa compared to that of 126 ± 1 MPa in air.

**4.2. Cross-Linking.** The hydrogel particle's rigidity can be efficiently tuned by changing the cross-link density of a network., *i.e.*, the number of cross-link bonds per unit volume. A network can contain either physical (temporary) or chemical (permanent) cross-link bonds or a combination of those. The number and type of the cross-link bonds can control the network elasticity and reversibility of the elastic response.

Varied rigidity of hydrogel micro- and nanoparticles by increased cross-link density was demonstrated for 150 nm[69] and 800−1000 nm[82] hydrogel nanoparticles made of *N*,*N*-diethyl acrylamide and 2-hydroxyethyl methacrylate (HEMA) with the elasticity range of 35−136 kPa and 15−156 kPa, respectively. When the ratio between gelatin and the glutaraldehyde cross-linker was changed, more rigid 350 nm cationic nanogels were obtained with Young's modulus in the range from 630 to 3400 kPa.[83] Using zwitterionic poly(carboxybetaine methacrylate), zwitterionic nanogels with an average size of 120−200 nm and an elastic modulus in the range of 180−1350 kPa were synthesized by inverse microemulsion polymerization using a redox-sensitive L-cystine bis(acrylamide) cross-linker[69] or a carboxybetaine DA cross-linker to control blood circulation and biodistribution of the hydrogel nanoparticles.[84] Supersoft PEG hydrogel particles were synthesized from 8-arm-PEG using a bifunctional *N*-hydroxysuccinimide cross-linker. The particles exhibited an elastic moduli in the range from 0.2 to 3.3 kPa,[30] which is much lower compared to PEG nanoparticles obtained by PRINT technology (7.8−64 kPa)[24] or protein porous particles obtained through templating on sacrificial porous calcium carbonate and cross-linked with glutaraldehyde (∼4 kPa),[85] which is due to the low density of the supersoft PEG nanogels.

When *N*-isopropylacrylamide was copolymerized with styrene, the stiffness of the submicron microgels of polystyrene-*co*-PNIPAM could be significantly increased to the elastic modulus range from 300 to 700 MPa by controlling the amount of *N*,*N*′-methylene bis(acrylamide) cross-linker.[86]

Our group showed that nonspherical multilayer hydrogel capsules could be synthesized using the multilayer assembly of polymers on the surfaces of nonspherical sacrificial inorganic microparticles.[87−89] The rigidity of the capsule hydrogel shell can also be controlled by increasing the hydrogel shell's cross-link density. For example, we demonstrated that, in amine-containing copolymers of PMAA,[88,89] PVPON,[90] or poly(*N*-vinylcaprolactam) (PVCL)[91] obtained via free-radical copolymerization, the number of cross-links could be controlled by the molar ratio of monomer units with amine groups in the copolymer. By studying high-aspect-ratio discoidal capsules made of PMAA multilayer hydrogels, we showed that spherical $(PMAA)_{15}$ capsules displayed a dramatic 19-fold volume increase when solution acidity was increased from pH = 4 to pH = 7.4, while two-component $(PVPON/PMAA)_5$ capsules exhibited only 2.9-fold volume increase (Figure 5b−e).[88] This difference in pH-triggered capsule swelling was rationalized by comparing water uptake by the capsule hydrogel shell. The $(PMAA)_5$ multilayer hydrogel displayed a 2-fold greater water uptake than $(PMAA/PVPON)_5$ at pH = 3 with the water content of 41% and 19% for $(PMAA)_5$ and $(PMAA/PVPON)_5$, respectively.[88] The presence of the PVPON component reduced free volume in the dual-component network suppressing the capsule swelling and softness.

An elastic response can also be characterized by complete recovery of the capsule's original shape after stress removal, whereas a plastic response is accompanied by a permanent change of the capsule's shape, *e.g.*, irreversible buckling or capsule rapture. The shape loss due to osmotic buckling observed previously in ionically paired multilayer capsules is generally irreversible. Thus, for example, spherical ionically paired PSS/PAH multilayer capsules were irreversibly deformed (buckled) in response to the isotropic osmotic pressure from the added PSS macromolecules, which could not permeate the capsule shell. At the same time, water could diffuse through the semipermeable capsule shell.[46]

The type and density of bonds between the polymer chains in the capsule shell can affect the capsule's shape recovery after stress removal. Generally, a covalently linked network can manifest elastic behavior, while the secondary bonds (*e.g.*, hydrogen bonds or ionic pairs) lead to a viscoelastic hydrogel behavior. The persistence of the cross-links tightly holding the polymeric chains in the former confers a rubber-like behavior to the hydrogel, while breaking and reforming the links in the latter can dissipate energy and relax the structure. Thus, our works on pH-triggered shape change of cubical hydrogel capsules demonstrated that pH-induced swelling of the cubical $(PMAA)_{13}$ hydrogel capsule shell led to partial shape reversibility due to the presence of both covalent and ionic links in the network.[92] Conversely, the swelling-induced discoidal-to-ellipsoidal shape transformations of the $(PMAA)_{15}$ hydrogel capsules with only covalent links in the network showed a complete shape recovery.[88]

The rigidity of the multilayer hydrogel capsule shell is essential in capsule shape recovery. Thus, shape transitions from small-to-large cubical capsules of a more rigid $(PMAA-PVPON)_5$ hydrogel[88] were completely reversible, and the more rigid hydrogel could better withstand the stresses due to pH-triggered swelling. In contrast, the softer $(PMAA)_{20}$ single-component cubical capsule was subject to the outward bending of its side faces, and the changes were only partially reversible.[89] The difference in the two network types was that the former contains covalent cross-links and dynamic hydrogen bonding, while the latter contains only covalent linkages.

In a recent example, our group demonstrated that spherical hydrogen-bonded capsules, in which the polymer network is obtained through interpolymer hydrogen bonding-based complexation of polymers connected via physical links, can completely regain their original shape after the removal of osmotic pressure differences by rinsing out PSS macromolecules from the capsule solution.[47] The elasticity modulus of the (PMAA/PVPON) multilayer hydrogen-bonded capsules at pH = 3 was found to be 97 ± 8 MPa (characteristic for elastomeric networks) as analyzed via the osmotic pressure difference method.

Unlike solid particles, the stiffness of a hollow polymeric shell made of the same material with the same thickness


https://doi.org/10.1021/acsapm.1c00157
ACS Appl. Polym. Mater. 2021, 3, 2274−2289

depends on the capsule diameter since the capsule rigidity defined through the wall stiffness, $k$, is directly proportional to Young's modulus, $E$, and the wall thickness, $h$, but inversely proportional to the capsule size, $L$, and the Poisson ratio, $\nu$, as follows[93] (3)

$$k = \frac{4h^2E}{(L/2)\sqrt{3(1-\nu)^2}} \tag{3}$$

Therefore, when the capsule wall thickness or capsule size is varied, its rigidity can be easily controlled to control biological properties.[21,94] For example, the stiffness of the polyelectrolyte capsules made by the LbL assembly of anionic dextran sulfate and cationic poly(L-arginine) hydrochloride increased from 2 to 10 N/m when the number of the polymer bilayers within the capsule shell increased from 4 to 16.[94] Similarly, when three polymerized layers in hyaluronic acid (HA) capsules obtained by via one-step polymerization of HA macro-cross-linkers were added, the stiffness of the HA capsules increased almost linearly 3 times.[21] We demonstrated that the 15.5-bilayer hydrogen-bonded (PVPON/TA) multilayer capsules with 2-fold increased rigidity due to the drying-induced formation of capsule half-shells with a double-shell thickness were internalized 2-times better by THP-1 monocyte-derived macrophages.[60]

**4.3. Stimuli Dependence.** The physiologically relevant ranges of temperature and pH can be used as a guidance for developing polymeric particulates with controllable changes in their elasticity to facilitate the release of drugs or the interaction with cells in response to changes in the surrounding environment or physical treatment. For example, the pH values in the tumor microenvironment can vary in the range from 7 to 5.6,[95] so the particle stiffness can be varied in this range of pH to achieve a desirable change in particle rigidity to facilitate specific tissue targeting, preferential endothelial adhesion, and cellular internalization.

The pH-sensitive hydrogels can be useful in the development of polymeric carriers with the particle rigidity switchable in the physiological range. For example, the stiffness of the spherical PMAA multilayer hydrogel capsules increased from less than 1 to 550 ± 150 mN $m^{-1}$ when the solution pH was decreased from 6.5 to 5.4 as measured by AFM nanoindentation in solution (Figure 5f,g).[93] A similar stiffening trend was observed for less swellable (PMAA-PVPON) multilayer hydrogel capsules. They exhibited 18-fold increased stiffness in the interval of 7 < pH < 5.5 when solution pH was lowered.[93] The pH-induced change in the capsule rigidity was reversible and highly reproducible and resulted from decreased PMAA ionization and also in the dissociation of intermolecular hydrogen bonds in the case of a PMAA/PVPON capsule. These systems might be useful for a prolonged circulation in the blood due to their softness; however, their increased stiffness while inside a tumor environment with slightly lower acidity may facilitate a better adhesion and cellular uptake.

Since the pH of the healthy skin surface can vary from 4.7 to 5.1, while the average skin temperature is 34−37 °C,[96] the design of polymeric particles that can change their rigidity within these values in response to local changes or exogenous signals (*e.g.*, mild hyperthermia induced by heat or therapeutic ultrasound) may improve transdermal drug delivery as well as the drug release rate. In this case, the thermoresponsive polymers that show a sharp phase transition in the temperature range of 34−42 °C can benefit the development of polymeric particulates with temperature-triggered changes in rigidity. Most temperature-sensitive polymeric particles are currently synthesized from PNIPAM, which has a lower critical solution temperature in water at ∼32 °C. For example, PNIPAM microgel particles adsorbed on silica surfaces were shown to switch Young's modulus from 86 ± 17 to 330 ± 49 kPa when solution temperature was elevated from 25 to 37 °C (Figure 5h,i).[76] The surface-adsorbed microgels decreased their volume by 3-fold and were used for controlled spreading and detachment of mouse fibroblast cells. The submicron PNIPAM microgels obtained by Tagit and co-workers via surfactant-free emulsion radical polymerization were shown to decrease their size in solution from 550 nm to less than 300 nm at 25 and 40 °C, respectively, due to the PNIPAM chains collapse and water expulsion from the bulk of a particle.[81] Conversely, when they were adsorbed on the hydrophilic silica surface, the microgels increased their height while decreasing the area of adsorption at a temperature higher than its lower critical solution temperature (LCST) and demonstrated an increase in their Young's modulus in water from 1.8 to 12.8 MPa, above and below their volume phase transition temperature of 32 °C.[81]

Copolymerization of *N*-isopropylacrylamide (NIPAM) with acrylic acid (AA) in the presence of *N*,*N*′-methylene bis(acrylamide) via aqueous free-radical precipitation polymerization resulted in poly(NIPAM-*co*-AA) microgel particles of ∼1 μm. They could swell at pH > 4.5 due to acidic group deprotonation, electrostatic interchain repulsion, and increased osmotic pressure of the counterions.[97] In this case, the temperature-induced switching of particle elasticity could only be obtained at the lower pH of 3 with Young's moduli of 34 Pa at 25 °C and 505 Pa at 35 °C.[97]

The use of other temperature-sensitive polymers such as PVCL,[98] which has continuous LCST values in the range from 35 to 42 °C depending on molecular weight and concentration, can expand the opportunities for the development of polymeric drug delivery carriers with temperature-dependent particle volume and rigidity. For instance, PVCL-*co*-(aminopropyl) methacrylamide copolymers were used to synthesize cubical PVCL multilayer hydrogel capsules, which showed a 21% size shrinkage at ∼38−39 °C without a shape change, suggesting a possible stiffness increase at the elevated temperature.[91]

## 5. PARTICULATES WITH RIGIDITIES ANALOGOUS TO BLOOD CELLS

Many living cells have an outstanding ability to reverse deformation. For instance, the deformability of the human RBCs allows for their continuous circulation, while their increased rigidity can lead to numerous pathological states.[99] Therefore, RBCs' decreased deformability leads to their clearance from the bloodstream by splenic filtration. Subsequently, studies on the correlations between particle rigidity (responsible for its deformability and shape recovery) and its *in vivo* behavior, including circulation time, margination in the flow, and tissue accumulation, are necessary for the development of advanced vehicles for theranostic delivery and tissue targeting, which can mimic blood components including RBCs, white blood cells (WBCs), and platelets. Herein, we briefly review the approaches used to obtain RBC-mimicking polymeric carriers.

**5.1. Mimicking Blood Cell Elasticity.** Control of the cross-link density of polymer particles is among the main ways to tailor their rigidity to mimic the mechanical behavior of


https://doi.org/10.1021/acsapm.1c00157
ACS Appl. Polym. Mater. 2021, 3, 2274−2289

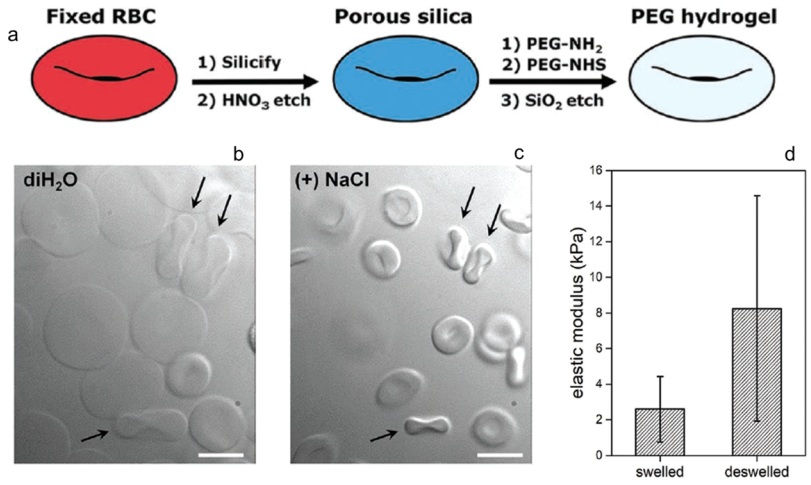


**Figure 6.** (a) PEG replicas of RBCs were synthesized by silicifying fixed RBCs, followed by etching of a cell template, PEG polymerization on a porous silica template, and silica etching. The PEG replicas of RBCs swollen in water (b) deswelled in 0.15 M NaCl solution (c). Arrows point to side-views of the PEG particles. (d) The elastic modulus of swelled and deswelled PEG particles. Reprinted with permission from ref 101. Copyright 2019 Wiley and Sons.

living cells.[30,100] For example, hydrogel RBC-like particles were obtained from PEG by coating a conformal layer of silica using a sol−gel process on the internal and external surfaces of chemically fixed cells, followed by infiltration and cross-linking of PEG precursors and silica dissolution (Figure 6).[101] The particles of a similar size but different elastic modulus from 5.51 ± 3.40 to 25.65 ± 20.61 kPa were produced by changing a cross-linker concentration from 0.625 to 1.25 mg $mL^{-1}$. However, higher cross-linker concentrations caused a significant variability in Young's moduli (73.23 ± 56.90 kPa), which followed the substantial, more than 100%, variation in elastic moduli characteristic for subpopulations of adipose-derived stem cells.

A series of PEGDA and 2-carboxyethyl acrylate (CEA) particles with a varied elasticity by varying the cross-linker concentration were synthesized by UV-initiated polymerization.[102] The hydrated shear modulus of these particles could be varied from 170 ± 40 to 7.7 ± 0.3 kPa for high and low cross-link densities, respectively, which was similar to that of RBCs.

Cross-linking of protein coating deposited using the LbL assembly on surfaces of RBC-shaped PLGA microparticles of 7 ± 2 μm synthesized via the electrohydrodynamic jetting process[48] was demonstrated to mimic a flexible shell of RBCs. The protein shell composed of either Hb/bovine serum albumin (Hb/BSA) or PAH/BSA was first deposited on the PLGA templates and cross-linked, and 9-layer protein capsules were obtained upon PLGA dissolution in 2-propanol/THF mixture. PLGA dissolution resulted in softening of the protein cross-linked shell, which had a Young's modulus of 92.8 ± 42 kPa by AFM indentation measurements.[48] This value is close to the Young's modulus of mouse RBCs (15.2 ± 3.5 kPa) and drastically lower than that of the original PLGA template (1.6 ± 0.6 GPa). These soft RBC protein replicas of 7 μm could reversibly deform while flown inside a capillary with a 5 μm diameter, recovering their original discoidal shape outside the capillary similarly to natural RBCs.

Besides, varying cross-link density using the PRINT technique allowed both the mechanical properties of hydrogel particles to be tailored and hydrogels with low mesh density for passive diffusion of molecules throughout the hydrogel to be produced. For example, highly deformable triethylene glycol acrylate-2-carboxyethyl acrylate particles with RBC shape and size made using the PRINT method were loaded with Hb for oxygen transportation.[103] The loading ratio of Hb controlled particle stiffness. The Hb−hydrogel particles were able to restore their initial disk shape after passing through the 50 μm long microfluidic pores of 3 μm in diameter at 60 μL/min at the Hb loading ratio of 2.8.[24] However, most of the stiffer particles with the Hb loading ratio of 5.1 were lodged at the pore entrances and unable to pass through the pores.

**5.2. Effect of Particle Rigidity on Margination in the Flow.** RBCs, white blood cells (WBCs), and platelets are known to have a different flow behavior in the bloodstream, *e.g.*, to show a different margination termed as the ability to migrate from the central flow toward the vessel wall.[104] RBCs do not marginate in healthy blood, while the WBCs and platelets flow to the wall more efficiently, which was attributed to the WBCs and platelets being significantly stiffer and more rigid than RBCs (the RBC Young's modulus is 26 ± 7 kPa).[105] Hydrodynamic simulation studies of carriers in blood flow found that more deformable, softer particles will not generally marginate, unlike their rigid counterparts.[105,106]

In mimicking natural blood cell margination that can allow for effective microvasculature targeting, the interplay between deformability and stiffness is crucial to replicate the RBC flow behavior.[33,107] Pinho et al. demonstrated the use of poly(dimethylsiloxane) (PDMS) as an excellent material to produce microparticles with deformability similar to human RBCs.[108] Spherical PDMS microparticles fabricated by mixing PDMS elastomer with a curing agent at varying ratios exhibited migration toward the microfluidic channel walls similar to that of unhealthy, more rigid RBCs. Deformation of both PDMS microparticles and RBCs was found to increase at larger flow rates, with PDMS particles exhibiting the deformation in the range between healthy and pathological RBCs. However, no dependence of PDMS deformation on the curing agent concentration was found. Conversely, RBCs' shape recovery time was higher than that of the PDMS particles attributed to the RBCs' biomechanical properties.


https://doi.org/10.1021/acsapm.1c00157
ACS Appl. Polym. Mater. 2021, 3, 2274−2289

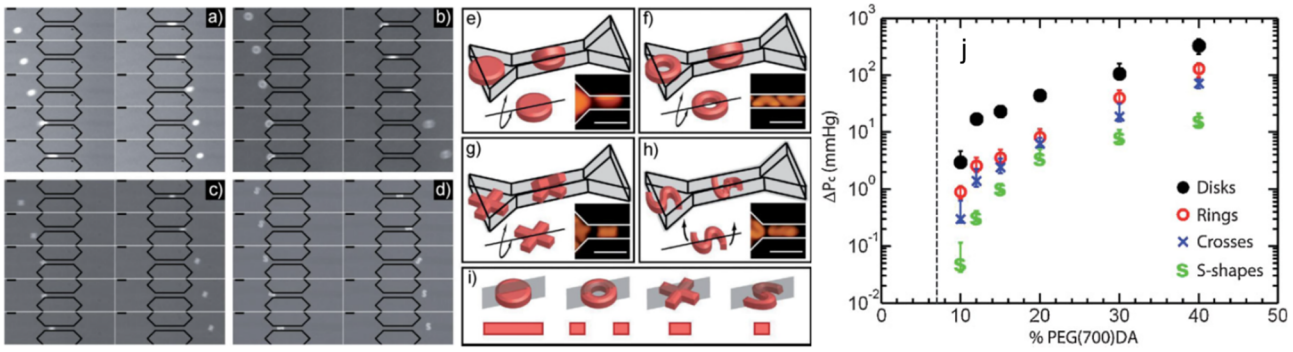


**Figure 7.** Images (a–d) of PEG particles in the shape of disks, rings, crosses, and S-shapes passing through a 4 $\mu$m channel. (e–h) Schematics with optical image inserts show the deformation states of disks (e), rings (f), crosses (g), and S-shapes (h). (i) Schematics of the planes where deformation occurs for each particle with the particles' cross sections in those planes. (j) Critical pressure differentials at which the particles pass through the channel as a function of the PEGDA concentration. Reprinted with permission from ref 34. Copyright 2010 Wiley and Sons.

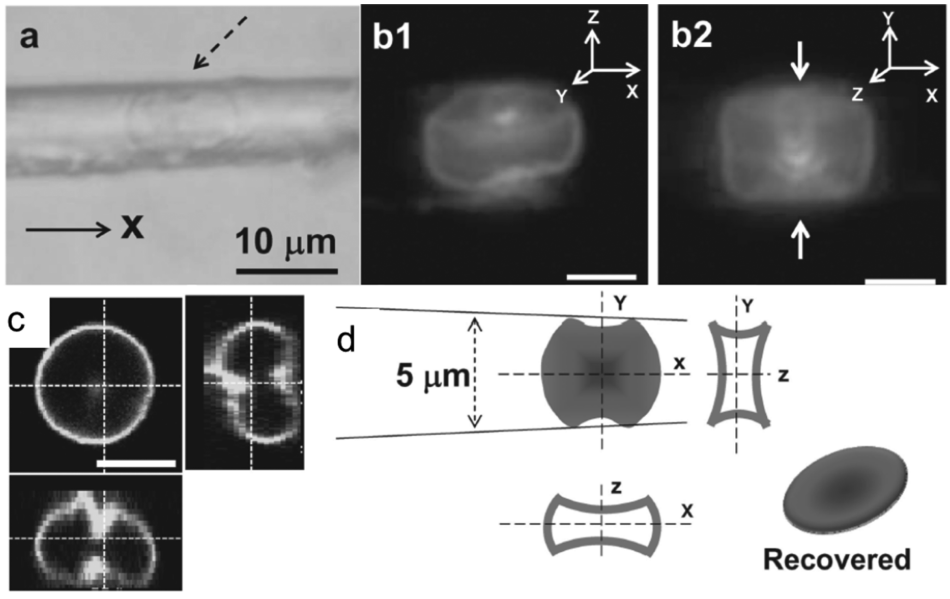


**Figure 8.** (a) Optical image of a PAH hydrogel capsule of the RBC shape in the 5 $\mu$m capillary. Fluorescence images of the capsule inside the capillary: a side view (b1) and a view from the capillary orifice (b2). (c) Three-dimensional reconstruction of the microcapsule when it passed through the channel. (d) Schematics show the deformation of the PAH hydrogel capsule inside the capillary and its recovery. Scale bars in (b, c) are 5 $\mu$m. Reprinted with permission from ref 36. Copyright 2013 Wiley and Sons.

## 6. EFFECT OF PARTICLE SHAPE

Compared to spherical particles, mechanical properties of nonspherical soft particulates have been much less investigated and mainly include those where particle geometry and stiffness are varied independently.[56,109] There are much fewer studies on the comparative impact of nonspherical shape in which particle shape is systematically varied while composition and size remain the same. The main challenges in the fabrication of soft colloids with complex geometries and monodisperse size are the synthetic difficulties of scale-up. Another challenge might be the quantification of rigidity in particulates of the nano- and micrometer sizes. However, as the studies below illustrate, the particle shape might be a powerful tool to control particle mechanical behavior.

Haghgooie et al. showed that the hydrogel vehicle's shape could regulate the hydrogel particle's mechanical property defined as deformability, *i.e.*, the ability of a particle to change and restore shape while passing through a microchannel, necessary to navigate through constrictions of blood vasculature under pressure differentials observed in human capillaries.[34] In that study, 8 $\mu$m sized disks, rings, crosses, and S-shapes were obtained by polymerizing PEGDA, and different pressure-induced deformability was demonstrated when passing through a 4 $\mu$m microfluidic channel with various pressure differentials. Among those, disk-shaped microgels were the least deformable, followed by rings, crosses, and S-shapes. The difference in the hydrogel deformability was attributed to a shape-controlled mode of passage. For example, disks, rings, and crosses preferred to buckle, rather than compress during their passage, while S-shapes twisted to pass through the narrow channel (Figure 7).[34]

DeSimone and colleagues studied deformability of PEGDA particles of a filamentous shape passing through membranes with 0.2 $\mu$m pores and found that particles with the highest aspect ratio, 80 × 5000 nm, showed the lowest percentage of shape recovery.[110] Those hydrogel particles were prepared by PRINT soft lithography and had a varied aspect ratio with a constant width of 80 nm and lengths ranging from 180 to 5000 nm.


https://doi.org/10.1021/acsapm.1c00157
ACS Appl. Polym. Mater. 2021, 3, 2274–2289

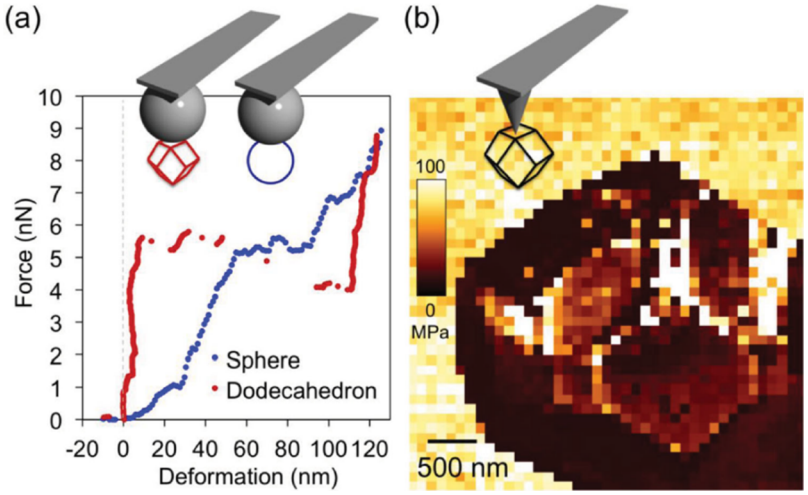


**Figure 9.** (a) Force-deformation curves for comparing the stiffness of the spherical and rhombic dodecahedral PSS/PAH multilayer capsules of the same size and shell thickness as analyzed by AFM nanoindentation using colloidal probes. (b) Two-dimensional force map of a rhombic dodecahedral capsule in aqueous solution. Reprinted with permission from ref 111. Copyright 2013 Wiley and Sons.

Investigations of mechanical stability of shaped LbL capsules have also been limited to a few studies. Gao and collaborators showed that nonspherical hydrogel capsules of PAH cross-linked with glutaraldehyde had a better shape recovery compared to their spherical counterparts after a pressure-induced shape loss (Figure 8).[36] Specifically, 90% of 7 $\mu$m discoidal $(PAH)_{10}$ capsules recovered their shape when passing through a 5 $\mu$m glass capillary, while spherical capsules of the same composition and size showed only 63% recovery ratio. Conversely, our group illustrated that both cubical and spherical 2 $\mu$m capsules prepared from hydrogen-bonded (TA/PVPON) multilayers successfully extravasated through much smaller 0.8 $\mu$m membrane pores under 18 psi pressure and were able to recover their shape (Figure 3e–h).[35]

Several groups showed that LbL capsules with vertices and edges demonstrated increased structural rigidity and better mechanical stability against compressive stresses than spheres. The enhanced mechanical properties of anisotropic capsules imply that faceting can be a powerful tool to control the polymer colloids' mechanical properties. The Caruso and Granick groups explored faceted ionically paired PSS/PAH microcapsules using AFM compression and found that rhombic dodecahedral microcapsules with 12 congruent faces had enhanced stiffness ($292 \pm 73$ mN $m^{-1}$) compared to spherical capsules of the same size and shell thickness ($76 \pm 21$ mN $m^{-1}$) (Figure 9).[111] Similarly, a computational study performed by the Tsukruk and Alexeev groups suggested that cubical and tetrahedral TA/PVPON multilayer microcapsules are expected to exhibit increased mechanical stability upon a decrease of internal pressure in the solution due to inhomogeneous strain–stress distributions along the sharp corners and edges of the cube.[15] The results indicate that sharp edges and vertices act as reinforcing frames against random buckling compared to more easily buckled spherical microcapsules. Indeed, in our work with cubical $(TA/PVPON)_{15.5}$ capsules, we demonstrated that the dried capsules buckled with the cubic faces collapsed inside the capsule volume with a few cube edges bent as well.[60]

Conversely, Tsukruk and collaborators found that TA/PVPON cubical capsules prepared on cadmium carbonate sacrificial templates were softer than their spherical counterparts made on $SiO_2$ templates.[112] On the basis of the surface force spectroscopy analysis, spherical capsules were 5-fold more rigid with a Young's moduli of $4.3 \pm 0.4$ and $0.8 \pm 0.4$ MPa for spheres and cubes, respectively. The stiffness difference was attributed to cores with different surface properties and dissolution mechanisms, leading to more porous shells in cubical capsules.[112]

Other types of nonspecial shapes also showed mechanical properties to be different from that characteristic for spheres. Thus, for example, hydrogel capsules made by the LbL assembly demonstrated a different deformation behavior in contrast to filled (continuous) hydrogel particles with more extensive flexibility than a filled hydrogel of the same shape. The 7 $\mu$m discoidal PAH capsules cross-linked with glutaraldehyde squeezed through a 5 $\mu$m glass capillary tip and recovered their original shape.[36] Notably, this discoidal capsule's elasticity modulus was in the order of hundreds of MPa, which is much larger than the passage threshold for the filled discoidal PRINT hydrogels.[113] This difference was attributed to the hollow capsule interior mimicking RBC with fluid wrapped by a flexible membrane. A flexible membrane can facilitate better shape deformation and recovery via fluid-like deformation of the capsule shell, unlike continuous hydrogels, which may have difficulty facilitating such large displacements.

## 7. CONCLUSION

The rigidity of a polymeric therapeutic carrier is among the key physical factors affecting the biological behavior of cells. To advance the development of polymeric particulates with tunable rigidity and programmed mechanical behavior in the bloodstream, a better understanding of the effects of a carrier's mechanical clues on the regulation of various biological phenomena is crucial. During the last two decades, the fundamental knowledge related to the effects of particle rigidity on cellular internalization, tissue accumulation, and behavior in the flow have been accumulated, and a toolbox of analytical approaches to observe and quantify the particles' deformability and elastic properties, including microfluidics, filtration measurements, and AFM nanoindentation, has been established. Also, computational studies have been attempted to describe the complexity of endocytosis and flow mechanics of


https://doi.org/10.1021/acsapm.1c00157
ACS Appl. Polym. Mater. 2021, 3, 2274–2289

polymeric particulates. However, these findings raise many essential questions about the synthesis and applications of polymeric particulate materials with controlled rigidity that need to be addressed in future studies. Since various cells demonstrate a broad spectrum of responses toward the particulates' mechanical aspects, the ranges of optimal rigidity values need to be established to control the cell biological responses. Thus, synthetic and engineering methods need to be developed to scale up particle fabrication with reduced manufacturing costs. Especially challenging is the production of soft particulates with low elasticity and reproducible mechanical responses in large quantities. The interplay between the particles' shape and rigidity is a novel and intriguing research area since the exploration of the effects of induced stresses on the particle shape in the flow could bring new insights into cell−particle interactions in natural biological environments. In this respect, more diverse and robust polymeric structures capable of the elastic change on demand would vastly broaden our capabilities to control biological responses. Since low rigidity and large particulates are known to decrease their internalization by cells, switching to smaller and more rigid particles by utilizing pH- and temperature-responsive polymeric systems could increase particle uptake by the cells. When one expands the rigidity switch triggers to ultrasound and light, this research area can be brought closer to the more relevant clinical environment applications. Nonspherical shapes can offer larger surface areas to be used for cell targeting and introduce new aspects of controlling particle rigidity by varying shapes. In this regard, theoretical modeling on shape-induced rigidity will be critical to support experimental and applied research in this area. On the other hand, computational research should be supported by *in vivo* biodistribution studies and by the development of new instrumental approaches with a high spatial−temporal resolution to visualize particle deformations in the flow and during cell interaction and intracellular trafficking. We believe that exploring the rigidity-controlled properties of polymer particles and their behavior in the biological environment will advance a fundamental understanding of the properties of soft polymeric colloids and broaden these materials' applications in the biomedical field.

## AUTHOR INFORMATION


### Corresponding Author

**Eugenia Kharlampieva** − *Department of Chemistry, Center for Nanomaterials and Biointegration, and O'Neal Comprehensive Cancer Center, The University of Alabama at Birmingham, Birmingham, Alabama 35294, United States;* orcid.org/0000-0003-0227-0920; Email: ekharlam@uab.edu

### Authors

**Veronika Kozlovskaya** − *Department of Chemistry, The University of Alabama at Birmingham, Birmingham, Alabama 35294, United States;* orcid.org/0000-0001-9089-4842

**Maksim Dolmat** − *Department of Chemistry, The University of Alabama at Birmingham, Birmingham, Alabama 35294, United States*

Complete contact information is available at: https://pubs.acs.org/10.1021/acsapm.1c00157


### Notes

The authors declare no competing financial interest.

## ACKNOWLEDGMENTS

This work was supported by the National Science Foundation NSF-DMR Award #1904816.

## REFERENCES


(1) Anselmo, A. C.; Mitragotri, S. Impact of Particle Elasticity on Particle-Based Drug Delivery Systems. *Adv. Drug Delivery Rev.* **2017**, *108*, 51−67.

(2) Ina, M.; Cao, Z.; Vatankhah-Varnoosfaderani, M.; Everhart, M. H.; Daniel, W. F. M.; Dobrynin, A. V.; Sheiko, S. S. From Adhesion to Wetting: Contact Mechanics at the Surfaces of Super-Soft Brush-Like Elastomers. *ACS Macro Lett.* **2017**, *6*, 854−858.

(3) Myerson, J. W.; Anselmo, A. C.; Liu, Y.; Mitragotri, S.; Eckmann, D. M.; Muzykantov, V. R. Non-Affinity Factors Modulating Vascular Targeting of Nano- and Microcarriers. *Adv. Drug Delivery Rev.* **2016**, *99*, 97−112.

(4) Palomba, R.; Palange, A. L.; Rizzuti, I. F.; Ferreira, M.; Cervadoro, A.; Barbato, M. G.; Canale, C.; Decuzzi, P. Modulating Phagocytic Cell Sequestration by Tailoring Nanoconstruct Softness. *ACS Nano* **2018**, *12*, 1433−1444.

(5) Danielsen, S. P. O.; Beech, H. K.; Wang, S.; El-Zaatari, B. M.; Wang, X.; Sapir, L.; Ouchi, T.; Wang, Z.; Johnson, P. N.; Hu, Y.; Lundberg, D. J.; Stoychev, G.; Craig, S. L.; Johnson, J. A.; Kalow, J. A.; Olsen, B. D.; Rubinstein, M. Molecular Characterization of Polymer Networks. *Chem. Rev.* **2021**, DOI: 10.1021/acs.chemrev.0c01304.

(6) Paulick, M.; Morgeneyer, M.; Kwade, A. A new method for the determination of particle contact stiffness. *Granular Matter* **2015**, *17*, 83−93.

(7) Caccavo, D.; Cascone, S.; Lamberti, G.; Barba, A. A. Hydrogels: Experimental Characterization and Mathematical Modelling of Their Mechanical and Diffusive Behavior. *Chem. Soc. Rev.* **2018**, *47*, 2357−2373.

(8) Yashchenok, A.; Parakhonskiy, B.; Donatan, S.; Kohler, D.; Skirtach, A.; Möhwald, H. Polyelectrolyte Multilayer Microcapsules Templated on Spherical, Elliptical and Square Calcium Carbonate Particles. *J. Mater. Chem. B* **2013**, *1*, 1223−1228.

(9) Decher, G., Schlenoff, J. B., Eds. *Multilayer thin films: Sequential assembly of nanocomposite materials*, 2nd ed.; Wiley & Sons, 2012.

(10) Cui, J.; Richardson, J. J.; Björnmalm, M.; Faria, M.; Caruso, F. Nanoengineered templated polymer particles: Navigating the biological realm. *Acc. Chem. Res.* **2016**, *49*, 1139−1148.

(11) Costa, R. R.; Mano, J. F. Polyelectrolyte Multilayered Assemblies in Biomedical Technologies. *Chem. Soc. Rev.* **2014**, *43*, 3453−3479.

(12) Pavlukhina, S.; Sukhishvili, S. A. Polymer Assemblies for Controlled Delivery of Bioactive Molecules from Surfaces. *Adv. Drug Delivery Rev.* **2011**, *63*, 822−836.

(13) Rao, J. P.; Geckeler, K. E. Polymer Nanoparticles: Preparation Techniques and Size-Control Parameters. *Prog. Polym. Sci.* **2011**, *36*, 887−913.

(14) Lisunova, M. O.; Drachuk, I.; Shchepelina, O. A.; Anderson, K. D.; Tsukruk, V. V. Direct Probing of Micromechanical Properties of Hydrogen-Bonded Layer-by-Layer Microcapsule Shells with Different Chemical Compositions. *Langmuir* **2011**, *27*, 11157−11165.

(15) Shchepelina, O.; Kozlovskaya, V.; Kharlampieva, E.; Mao, W.; Alexeev, A.; Tsukruk, V. V. Anisotropic Micro- and Nano-Capsules. *Macromol. Rapid Commun.* **2010**, *31*, 2041−2046.

(16) Ghaemi, A.; Philipp, A.; Bauer, A.; Last, K.; Fery, A.; Gekle, S. Mechanical Behavior of Microcapsules and Their Rupture under Compression. *Chem. Eng. Sci.* **2016**, *142*, 236−243.

(17) Perry, J. L.; Herlihy, K. P.; Napier, M. E.; DeSimone, J. M. PRINT: A novel platform toward shape and size specific nanoparticle theranostics. *Acc. Chem. Res.* **2011**, *44*, 990−998.

(18) Champion, J. A.; Katare, Y. K.; Mitragotri, S. Making Polymeric Micro- and Nanoparticles of Complex Shapes. *Proc. Natl. Acad. Sci. U. S. A.* **2007**, *104*, 11901−11904.
(19) Tao, L.; Zhao, X. M.; Gao, J. M.; Hu, W. Lithographically Defined Uniform Worm-Shaped Polymeric Nanoparticles. *Nanotechnology* **2010**, *21*, 095301.
(20) Vatankhah-Varnosfaderani, M.; Keith, A. N.; Cong, Y.; Liang, H.; Rosenthal, M.; Sztucki, M.; Clair, C.; Magonov, S.; Ivanov, D. A.; Dobrynin, A. V.; Sheiko, S. S. Chameleon-like Elastomers with Molecularly Encoded Strain-Adaptive Stiffening and Coloration. *Science* **2018**, *359*, 1509−1513.
(21) Sun, H.; Wong, E. H.; Yan, Y.; Cui, J.; Dai, Q.; Guo, J.; Qiao, G. G.; Caruso, F. The role of Capsule Stiffness on Cellular Processing. *Chem. Sci.* **2015**, *6*, 3505−3514.
(22) Vatankhah-Varnosfaderani, M.; Daniel, W. F. M.; Everhart, M. H.; Pandya, A. A.; Liang, H.; Matyjaszewski, K.; Dobrynin, A. V.; Sheiko, S. S. Mimicking Biological Stress-Strain Behaviour with Synthetic Elastomers. *Nature* **2017**, *549*, 497−501.
(23) Anselmo, A. C.; Zhang, M.; Kumar, S.; Vogus, D. R.; Menegatti, S.; Helgeson, M. E.; Mitragotri, S. Elasticity of Nanoparticles Influences Their Blood Circulation, Phagocytosis, Endocytosis, and Targeting. *ACS Nano* **2015**, *9*, 3169−3177.
(24) Merkel, T. J.; Jones, S. W.; Herlihy, K. P.; Kersey, F. R.; Shields, A. R.; Napier, M.; Luft, J. C.; Wu, H.; Zamboni, W. C.; Wang, A. Z.; Bear, J. E.; DeSimone, J. M. Using Mechanobiological Mimicry of Red Blood Cells to Extend Circulation Times of Hydrogel Microparticles. *Proc. Natl. Acad. Sci. U. S. A.* **2011**, *108*, 586−591.
(25) Xu, S. Q.; Nie, Z. H.; Seo, M.; Lewis, P.; Kumacheva, E.; Stone, H. A.; Garstecki, P.; Weibel, D. B.; Gitlin, I.; Whitesides, G. M. Generation of Monodisperse Particles by Using Microfluidics: Control over Size, Shape, and Composition. *Angew. Chem., Int. Ed.* **2005**, *44*, 724−728.
(26) Geissler, M.; Xia, Y. N. Patterning: Principles and Some New Developments. *Adv. Mater.* **2004**, *16*, 1249−1269.
(27) Tanaka, T.; Fillmore, D. J. Kinetics of Swelling of Gels. *J. Chem. Phys.* **1979**, *70*, 1214−1218.
(28) Li, Z.; Xiao, C.; Yong, T.; Li, Z.; Gan, L.; Yang, X. Influence of Nanomedicine Mechanical Properties on Tumor Targeting Delivery. *Chem. Soc. Rev.* **2020**, *49*, 2273−2290.
(29) Wu, P.-H.; Aroush, D. R.-B.; Asnacios, A.; Chen, W.-C.; Dokukin, M. E.; Doss, B. L.; Durand-Smet, P.; Ekpenyong, A.; Guck, J.; Guz, N. V.; Janmey, P. A.; Lee, J. S. H.; Moore, N. M.; Ott, A.; Poh, Y.-C.; Ros, R.; Sander, M.; Sokolov, I.; Staunton, J. R.; Wang, N.; Whyte, G.; Wirtz, D. A Comparison of Methods to Assess Cell Mechanical Properties. *Nat. Methods* **2018**, *15*, 491−498.
(30) Cui, J.; Björnmalm, M.; Liang, K.; Xu, C.; Best, J. P.; Zhang, X.; Caruso, F. Super-Soft Hydrogel Particles with Tunable Elasticity in a Microfluidic Blood Capillary Model. *Adv. Mater.* **2014**, *26*, 7295−7299.
(31) Voudouris, P.; Florea, D.; van der Schoot, P.; Wyss, H. M. Micromechanics of Temperature Sensitive Microgels: Dip in the Poisson Ratio Near the LCST. *Soft Matter* **2013**, *9*, 7158−7166.
(32) She, S.; Xu, C.; Yin, X.; Tong, W.; Gao, C. Shape Deformation and Recovery of Multilayer Microcapsules after Being Squeezed through a Microchannel. *Langmuir* **2012**, *28*, 5010−5016.
(33) Sun, H.; Björnmalm, M.; Cui, J.; Wong, E. H.; Dai, Y.; Dai, Q.; Qiao, G. G.; Caruso, F. Structure Governs the Deformability of Polymer Particles in a Microfluidic Blood Capillary Model. *ACS Macro Lett.* **2015**, *4*, 1205−1209.
(34) Haghgooie, R.; Toner, M.; Doyle, P. S. Squishy Non-Spherical Hydrogel Microparticles. *Macromol. Rapid Commun.* **2010**, *31*, 128−134.
(35) Alexander, J. F.; Kozlovskaya, V.; Chen, J.; Kuncewicz, T.; Kharlampieva, E.; Godin, B. Cubical Shape enhances the Interaction of Layer-by-Layer Polymeric Particles with Breast Cancer Cells. *Adv. Healthcare Mater.* **2015**, *4*, 2657−2666.
(36) She, S.; Li, Q.; Shan, B.; Tong, W.; Gao, C. Fabrication of Red-Blood-Cell-Like Polyelectrolyte Microcapsules and Their Deformation and Recovery Behavior Through a Microcapillary. *Adv. Mater.* **2013**, *25*, 5814−5818.
(37) Zhang, X.W.; Tao, Z.; Zhang, Q.M. Dynamic Behaviors of Visco-Elastic Thin-walled Spherical Shells Impact onto a Rigid Plate. *LAJSS* **2014**, *11*, 2607−2623.
(38) Li, Y.; Sarıyer, O. S.; Ramachandran, A.; Panyukov, S.; Rubinstein, M.; Kumacheva, E. Universal behavior of hydrogels confined to narrow capillaries. *Sci. Rep.* **2015**, *5*, 17017.
(39) Lulevich, V. V.; Andrienko, D.; Vinogradova, O. I. Elasticity of Polyelectrolyte Multilayer Microcapsules. *J. Chem. Phys.* **2004**, *120*, 3822−3826.
(40) Jaskiewicz, K.; Makowski, M.; Kappl, M.; Landfester, K.; Kroeger, A. Mechanical Properties of Poly(dimethylsiloxane)-block-Poly(2-methyloxazoline) Polymersomes Probed by Atomic Force Microscopy. *Langmuir* **2012**, *28*, 12629−12636.
(41) Chen, J. Nanobiomechanics of Living Cells: A Review. *Interface Focus* **2014**, *4*, 20130055.
(42) Vargas-Pinto, R.; Gong, H.; Vahabikashi, A.; Johnson, M. The Effect of the Endothelial Cell Cortex on Atomic Force Microscopy Measurements. *Biophys. J.* **2013**, *105*, 300−309.
(43) Alsharif, N.; Eshaghi, B.; Reinhard, B.; Brown, K. Physiologically Relevant Mechanics of Biodegradable Polyester Nanoparticles. *Nano Lett.* **2020**, *20*, 7536−7542.
(44) Fery, A.; Weinkamer, R. Mechanical Properties of Micro- and Nanocapsules: Single-Capsule Measurements. *Polymer* **2007**, *48*, 7221−7235.
(45) Knoche, S.; Kierfeld, J. Osmotic Buckling of Spherical Capsules. *Soft Matter* **2014**, *10*, 8358−8369.
(46) Gao, G.; Donath, E.; Moya, S.; Dudnik, V.; Möhwald, H. Elasticity of hollow polyelectrolyte capsules prepared by the layer-by-layer technique. *Eur. Phys. J. E: Soft Matter Biol. Phys.* **2001**, *5*, 21−27.
(47) Gupta, N.; Kozlovskaya, V.; Dolmat, M.; Kharlampieva, E. Shape Recovery of Spherical Hydrogen-Bonded Multilayer Capsules after Osmotically Induced Deformation. *Langmuir* **2019**, *35*, 10910−10919.
(48) Doshi, N.; Zahr, A. S.; Bhaskar, S.; Lahann, J.; Mitragotri, S. Red Blood Cell-Mimicking Synthetic Biomaterial Particles. *Proc. Natl. Acad. Sci. U. S. A.* **2009**, *106*, 21495−21499.
(49) Yu, S. S.; Lau, C. M.; Thomas, S. N.; Jerome, W. J.; Maron, D. J.; Dickerson, J. H.; Hubbell, J. A.; Giorgio, T. D. Size- and Charge-Dependent Non-Specific Uptake of PEGylated Nanoparticles by Macrophages. *Int. J. Nanomed.* **2012**, *7*, 799−813.
(50) Sylvestre, M.; Crane, C. A.; Pun, S. H. Progress on Modulating Tumor-Associated Macrophages with Biomaterials. *Adv. Mater.* **2020**, *32*, 1902007.
(51) Benne, N.; van Duijn, J.; Kuiper, J.; Jiskoot, W.; Slütter, B. Orchestrating immune responses: How size, shape and rigidity affect the immunogenicity of particulate vaccines. *J. Controlled Release* **2016**, *234*, 124−134.
(52) Baranov, M. V.; Kumar, M.; Sacanna, S.; Thutupalli, S.; van den Bogaart, G. Modulation of Immune Responses by Particle Size and Shape. *Front. Immunol.* **2021**, *11*, 607945.
(53) Beningo, K. A.; Wang, Y. Fc-Receptor-Mediated Phagocytosis is Regulated by Mechanical Properties of the Target. *J. Cell Sci.* **2002**, *115*, 849−856.
(54) Key, J.; Palange, A. L.; Gentile, F.; Aryal, S.; Stigliano, C.; Di Mascolo, D.; De Rosa, E.; Cho, M.; Lee, Y.; Singh, J.; Decuzzi, P. Soft Discoidal Polymeric Nanoconstructs Resist Macrophage Uptake and Enhance Vascular Targeting in Tumors. *ACS Nano* **2015**, *9*, 11628−11641.
(55) Garapaty, A.; Champion, J. A. Tunable Particles Alter Macrophage Uptake Based on Combinatorial Effects of Physical Properties. *Bioeng. Transl. Med.* **2017**, *2*, 92−101.
(56) Brown, T. D.; Habibi, N.; Wu, D.; Lahann, J.; Mitragotri, S. Effect of Nanoparticle Composition, Size, Shape, and Stiffness on Penetration Across the Blood-Brain Barrier. *ACS Biomater. Sci. Eng.* **2020**, *6*, 4916−4928.
(57) Nowak, M.; Brown, T. D.; Graham, A.; Helgeson, M. E.; Mitragotri, S. Size, Shape, and Flexibility Influence Nanoparticle


https://doi.org/10.1021/acsapm.1c00157
ACS Appl. Polym. Mater. 2021, 3, 2274−2289

Transport across Brain Endothelium under Flow. *Bioeng. Transl. Med.* **2020**, *5*, e10153.
(58) Cui, J.; De Rose, R.; Best, J. P.; Johnston, A. P. R.; Alcantara, S.; Liang, K.; Such, G. K.; Kent, S. J.; Caruso, F. Mechanically Tunable, Self-Adjuvanting Nanoengineered Polypeptide Particles. *Adv. Mater.* **2013**, *25*, 3468−3472.
(59) Zheng, Y.; Xing, L.; Chen, L.; Zhou, R.; Wu, J.; Zhu, X.; Li, L.; Xiang, Y.; Wu, R.; Zhang, L.; Huang, Y. Tailored Elasticity Combined with Biomimetic Surface Promotes Nanoparticle Transcytosis to Overcome Mucosal Epithelial Barrier. *Biomaterials* **2020**, *262*, 120323.
(60) Chen, J.; Kozlovskaya, V.; Goins, A.; Campos-Gomez, J.; Saeed, M.; Kharlampieva, E. Biocompatible Shaped Particles from dried Multilayer Polymer Capsules. *Biomacromolecules* **2013**, *14*, 3830−3841.
(61) Yu, W.; Zhang, W.; Chen, Y.; Song, X.; Tong, W.; Mao, Z.; Gao, C. Cellular Uptake of Poly(allylamine hydrochloride) Microcapsules with Different Deformability and its Influence on Cell Functions. *J. Colloid Interface Sci.* **2016**, *465*, 149−157.
(62) Li, X.; Tang, H.; Huang, X.; Li, M.; Jiang, Z.; He, H.; Zhou, Z. Rigidity-Dependent Placental Cells Uptake of Silk-Based Microcapsules. *Macromol. Biosci.* **2019**, *19*, 1900105.
(63) Guo, P.; Liu, D.; Subramanyam, K.; Wang, B.; Yang, J.; Huang, J.; Auguste, D. T.; Moses, M. A. Nanoparticle Elasticity Directs Tumor Uptake. *Nat. Commun.* **2018**, *9*, 130.
(64) Stern, T.; Kaner, I.; Zer, N. L.; Shoval, H.; Dror, D.; Manevitch, Z.; Chai, L.; Brill-Karniely, Y.; Benny, O. Rigidity of Polymer Micelles Affects Interactions with Tumor Cells. *J. Controlled Release* **2017**, *257*, 40−50.
(65) Zhang, L.; Chen, H.; Xie, J.; Becton, M.; Wang, X. Interplay of Nanoparticle Rigidity and Its Translocation Ability through Cell Membrane. *J. Phys. Chem. B* **2019**, *123*, 8923−8930.
(66) Yu, M.; Xu, L.; Tian, F.; Su, Q.; Zheng, N.; Yang, Y.; Wang, J.; Wang, A.; Zhu, C.; Guo, S.; Zhang, X.; Gan, Y.; Shi, X.; Gao, H. Rapid Transport of Deformation-Tuned Nanoparticles across Biological Hydrogels and Cellular Barriers. *Nat. Commun.* **2018**, *9*, 2607.
(67) Sun, J.; Zhang, L.; Wang, J.; Feng, Q.; Liu, D.; Yin, Q.; Xu, D.; Wei, Y.; Ding, B.; Shi, X.; Jiang, X. Tunable Rigidity of (Polymeric Core)-(Lipid Shell) Nanoparticles for Regulated Cellular Uptake. *Adv. Mater.* **2015**, *27*, 1402−1407.
(68) Xia, Y.; Wu, J.; Wei, W.; Du, Y.; Wan, T.; Ma, X.; An, W.; Guo, A.; Miao, C.; Yue, H.; Li, S.; Cao, X.; Su, Z.; Ma, G. Exploiting the Pliability and Lateral Mobility of Pickering Emulsion for Enhanced Vaccination. *Nat. Mater.* **2018**, *17*, 187−194.
(69) Banquy, X.; Suarez, F.; Argaw, A.; Rabanel, J.-M.; Grutter, P.; Bouchard, J.-F.; Hildgen, P.; Giasson, S. Effect of Mechanical Properties of Hydrogel Nanoparticles on Macrophage Cell Uptake. *Soft Matter* **2009**, *5*, 3984−3991.
(70) Liang, Q.; Bie, N.; Yong, T.; Tang, K.; Shi, X.; Wei, Z.; Jia, H.; Zhang, X.; Zhao, H.; Huang, W.; Gan, L.; Huang, B.; Yang, X. The Softness of Tumor-Cell-Derived Microparticles Regulates Their Drug-Delivery Efficiency. *Nat. Biomed. Eng.* **2019**, *3*, 729−740.
(71) Zhang, L.; Cao, Z.; Li, Y.; Ella-Menye, J.-R.; Bai, T.; Jiang, S. Softer Zwitterionic Nanogels for Longer Circulation and Lower Splenic Accumulation. *ACS Nano* **2012**, *6* (8), 6681−6686.
(72) Coclite, A.; Pascazio, G.; de Tullio, M. D.; Decuzzi, P. Predicting the vascular adhesión of deformable drug carriers in narrow capillaries traversed by blood cells. *J. Fluids Struct.* **2018**, *82*, 638−650.
(73) Chen, X.; Cui, J.; Ping, Y.; Suma, T.; Cavalieri, F.; Besford, Q. A.; Chen, G.; Braunger, J. A.; Caruso, F. Probing Cell Internalization Mechanics with Polymer Capsules. *Nanoscale* **2016**, *8*, 17096−17101.
(74) Palankar, R.; Pinchasik, B.-E.; Schmidt, S.; De Geest, B.; Fery, A.; Möhwald, H.; Skirtach, A.; Delcea, M. Mechanical Strength and Intracellular Uptake of Caco3-Templated LbL Capsules Composed of Biodegradable Polyelectrolytes: The Influence of the Number of Layers. *J. Mater. Chem. B* **2013**, *1*, 1175−1181.
(75) Chen, X.; Cui, J.; Sun, H.; Müllner, M.; Yan, Y.; Noi, K. F.; Ping, Y.; Caruso, F. Analysing intracellular deformation of polymer capsules using structured illumination microscopy. *Nanoscale* **2016**, *8*, 11924−11931.
(76) Schmidt, S.; Zeiser, M.; Hellweg, T.; Duschl, C.; Fery, F.; Möhwald, H. Adhesion and Mechanical Properties of PNIPAM Microgel Films and Their Potential Use as Switchable Cell Culture Substrates. *Adv. Funct. Mater.* **2010**, *20*, 3235−3243.
(77) Tang, Z.; Akiyama, Y.; Okano, T. Recent Development of Temperature-Responsive Cell Culture Surface Using Poly(N-isopropylacrylamide). *J. Polym. Sci., Part B: Polym. Phys.* **2014**, *52*, 917−926.
(78) Best, J. P.; Yan, Y.; Caruso, F. The Role of Particle Geometry and Mechanics in the Biological Domain. *Adv. Healthcare Mater.* **2012**, *1*, 35−47.
(79) Leporatti, S.; Gerth, A.; Köhler, G.; Kohlstrunk, B.; Hauschildt, S.; Donath, E. Elasticity and Adhesion of Resting and Lipopolysaccharide-Stimulated Macrophages. *FEBS Lett.* **2006**, *580*, 450−454.
(80) Slaughter, B. V.; Khurshid, S. S.; Fisher, O. Z.; Khademhosseini, A.; Peppas, N. A. Hydrogels in Regenerative Medicine. *Adv. Mater.* **2009**, *21*, 3307−3329.
(81) Tagit, O.; Tomczak, N.; Vancso, G. J. Probing the Morphology and Nanoscale Mechanics of Single Poly(N-Isopropylacrylamide) Microgels across the Lower-Critical-Solution Temperature by Atomic Force Microscopy. *Small* **2008**, *4*, 119−126.
(82) Liu, W.; Zhou, X.; Mao, Z.; Yu, D.; Wang, B.; Gao, C. Uptake of Hydrogel Particles with Different Stiffness and its Influence on HepG2 Cell Functions. *Soft Matter* **2012**, *8*, 9235−9245.
(83) Zhang, W.; Han, B.; Lai, X.; Xiao, C.; Xu, S.; Meng, X.; Li, Z.; Meng, J.; Wen, T.; Yang, X.; Liu, J.; Xu, H. Stiffness of Cationized Gelatin Nanoparticles is a Key Factor Determining RNAi Efficiency in Myeloid Leukemia Cells. *Chem. Commun.* **2020**, *56*, 1255−1258.
(84) Zheng, Y.; Xing, L.; Chen, L.; Zhou, R.; Wu, J.; Zhu, X.; Li, L.; Xiang, Y.; Wu, R.; Zhang, L.; Huang, Y. Tailored Elasticity Combined with Biomimetic Surface Promotes Nanoparticle Transcytosis to Overcome Mucosal Epithelial Barrier. *Biomaterials* **2020**, *262*, 120323.
(85) Schmidt, S.; Behra, M.; Uhlig, K.; Madaboosi, N.; Hartmann, L.; Duschl, C.; Volodkin, D. Mesoporous Protein Particles Through Colloidal $CaCO_3$ Templates. *Adv. Funct. Mater.* **2013**, *23*, 116−123.
(86) Kruger, T.; Givens, B.; Lansakara, T.; Bell, K.; Mohapatra, H.; Salem, A.; Tivanski, A.; Stevens, L. Mechanosensitive Endocytosis of High-Stiffness, Submicron Microgels in Macrophage and Hepatocarcinoma Cell Lines. *ACS Appl. Bio Mater.* **2018**, *1*, 1254−1265.
(87) Kozlovskaya, V.; Xue, B.; Kharlampieva, E. Shape-Adaptable Polymeric Particles for Controlled Delivery. *Macromolecules* **2016**, *49*, 8373−8386.
(88) Kozlovskaya, V.; Alexander, J.; Wang, Y.; Kuncewicz, T.; Liu, X.; Godin, B.; Kharlampieva, E. Internalization of Red Blood Cell-mimicking Hydrogel Capsules with pH-triggered Shape Responses. *ACS Nano* **2014**, *8*, 5725−5737.
(89) Kozlovskaya, V.; Wang, Y.; Higgins, W.; Chen, J.; Chen, Y.; Kharlampieva, E. pH-Triggered Shape Response of Cubical Ultrathin Hydrogel Capsules. *Soft Matter* **2012**, *8*, 9828−9839.
(90) Higgins, W.; Kozlovskaya, V.; Alford, P. A.; Ankner, J. F.; Kharlampieva, E. Stratified Temperature-Responsive Multilayer Hydrogels of Poly(N-vinylpyrrolidone) and Poly(N-vinylcaprolactam): Effect of Hydrogel Architecture on Properties. *Macromolecules* **2016**, *49*, 6953−6964.
(91) Liang, X.; Kozlovskaya, V.; Chen, Y.; Zavgorodnya, O.; Kharlampieva, E. Thermosensitive Multilayer Hydrogels of Poly(N-vinylcaprolactam) as Nanothin Films and Shaped Capsules. *Chem. Mater.* **2012**, *24*, 3707−3719.
(92) Kozlovskaya, V.; Higgins, W.; Chen, J.; Kharlampieva, E. Switching Shape of Layer-by-Layer Hydrogel Microcontainers. *Chem. Commun.* **2011**, *47*, 8352−8354.
(93) Elsner, N.; Kozlovskaya, V.; Sukhishvili, S. A.; Fery, F. pH-Triggered Softening of Crosslinked Hydrogen-Bonded Capsules. *Soft Matter* **2006**, *2*, 966−972.


https://doi.org/10.1021/acsapm.1c00157
*ACS Appl. Polym. Mater.* 2021, 3, 2274−2289

(94) Hartmann, R.; Weidenbach, M.; Neubauer, M.; Fery, A.; Parak, W. J. Stifness-Dependent in Vitro Uptake and Lysosomal Acidification of Colloidal Particles. *Angew. Chem., Int. Ed.* **2015**, *54*, 1365−1368.
(95) Boedtkjer, E.; Pedersen, S. F. The Acidic Tumor Microenvironment as a Driver of Cancer. *Annu. Rev. Physiol.* **2020**, *82*, 103−126.
(96) Lambers, H.; Piessens, S.; Bloem, A.; Pronk, H.; Finkel, P. Natural Skin surface pH is on Average Below 5, Which is Beneficial for its Resident Flora. *Int. J. Cosmet. Sci.* **2006**, *28*, 359−370.
(97) Wiedemair, J.; Serpe, M. J.; Kim, J.; Masson, J.-F.; Lyon, L. A.; Mizaikoff, B.; Kranz, C. In-Situ AFM Studies of the Phase-Transition Behavior of Single Thermoresponsive Hydrogel Particles. *Langmuir* **2007**, *23*, 130−137.
(98) Kozlovskaya, V.; Kharlampieva, E. Self-Assemblies of Thermoresponsive Poly(N-vinylcaprolactam) Polymers for Applications in Biomedical Field. *ACS Applied Polym. Mater.* **2020**, *2*, 26−39.
(99) Mebius, R. E.; Kraal, G. Structure and Function of the Spleen. *Nat. Rev. Immunol.* **2005**, *5*, 606−616.
(100) Labriola, N. R.; Mathiowitz, E.; Darling, E. M. Fabricating Polyacrylamide Microbeads by Inverse Emulsification to Mimic the Size and Elasticity of Living Cells. *Biomater. Sci.* **2017**, *5*, 41−45.
(101) Meyer, K.; Labriola, N.; Darling, E.; Kaehr, B. Shape-Preserved Transformation of Biological Cells into Synthetic Hydrogel Microparticles. *Adv. Biosyst.* **2019**, *3*, 1800285.
(102) Fish, M.; Fromen, C.; Lopez-Cazares, G.; Golinski, A.; Scott, T.; Adili, R.; Holinstat, M.; Eniola-Adefeso, O. Exploring Deformable Particles in Vascular-Targeted Drug Delivery: Softer is Only Sometimes Better. *Biomaterials* **2017**, *124*, 169−179.
(103) Chen, K.; Merkel, T.; Pandya, A.; Napier, M.; Luft, J.; Daniel, W.; Sheiko, S.; DeSimone, J. Low Modulus Biomimetic Microgel Particles with High Loading of Hemoglobin. *Biomacromolecules* **2012**, *13*, 2748−2759.
(104) Kumar, A.; Graham, M. D. Margination and Segregation in Confined Flows of Blood and Other Multicomponent Suspensions. *Soft Matter* **2012**, *8*, 10536−10548.
(105) Kumar, A.; Rivera, R. G. H.; Graham, M. D. Flow-Induced Segregation in Confined Multicomponent Suspensions: Effects of Particle Size and Rigidity. *J. Fluid Mech.* **2014**, *738*, 423−462.
(106) Müller, K.; Fedosov, D. A.; Gompper, G. Understanding Particle Margination in Blood Flow - A Step toward Optimized Drug Delivery Systems. *Med. Eng. Phys.* **2016**, *38*, 2−10.
(107) Pinho, D.; Campo-Deaño, L.; Lima, R.; Pinho, F. T. In vitro Particulate Analogue Fluids for Experimental Studies of Rheological and Hemorheological Behavior of Glucose-Rich RBC Suspensions. *Biomicrofluidics* **2017**, *11*, 054105.
(108) Pinho, D.; Muñoz-Sánchez, B.; Anes, C.; Vega, E.; Lima, R. Flexible PDMS Microparticles To Mimic Rbcs In Blood Particulate Analogue Fluids. *Mech. Res. Commun.* **2019**, *100*, 103399.
(109) Liu, N.; Becton, M.; Zhang, L.; Wang, X. Mechanism of Coupling Nanoparticle Stiffness with Shape for Endocytosis: From Rodlike Penetration to Wormlike Wriggling. *J. Phys. Chem. B* **2020**, *124*, 11145−11156.
(110) Kersey, F. R.; Merkel, T. J.; Perry, J. L.; Napier, m. E.; DeSimone, J. M. Effect of Aspect Ratio and Deformability on Nanoparticle Extravasation through Nanopores. *Langmuir* **2012**, *28*, 8773−8781.
(111) Ejima, H.; Yanai, N.; Best, J. P.; Sindoro, M.; Granick, S.; Caruso, F. Near-Incompressible Faceted Polymer Microcapsules from Metal-Organic Framework Templates. *Adv. Mater.* **2013**, *25*, 5767−5771.
(112) Shchepelina, O.; Lisunova, M. O.; Drachuk, I.; Tsukruk, V. V. Morphology and Properties of Microcapsules with Different Core Releases. *Chem. Mater.* **2012**, *24*, 1245−1254.
(113) Merkel, T. J.; Chen, K.; Jones, S. W.; Pandya, A. A.; Tian, S.; Napier, M. E.; Zamboni, W. E.; DeSimone, J. M. The Effect of Particle Size on the Biodistribution of Low-Modulus Hydrogel PRINT Particles. *J. Controlled Release* **2012**, *162*, 37−44.


https://doi.org/10.1021/acsapm.1c00157
*ACS Appl. Polym. Mater.* 2021, 3, 2274−2289